HEAT TRANSFER ANALYSIS OF A PULSE DETONATION ENGINE

by

NEELIMA KALIDINDI

Presented to the Faculty of the Graduate School of
The University of Texas at Arlington in Partial Fulfillment
of the Requirements
for the Degree of

MASTER OF SCIENCE IN MECHANICAL ENGINEERING

THE UNIVERSITY OF TEXAS AT ARLINGTON
DECEMBER 2009

ACKNOWLEDGEMENTS

It is a pleasure to thank those who made this thesis possible with their support and encouragement which helped me to reach this milestone in my life. First, I would like to take this opportunity to thank my supervising advisor Dr. Frank Lu, Professor and Director of Aerodynamics Research Center, who has been abundantly helpful and assisted me in numerous ways. With his enthusiasm, his inspiration and his great efforts to explain things clearly and simply, he helped me in making my thesis easier. Throughout my thesis, he provided sound advice, encouragement, good company with lot of good ideas and remarkable patience.

Secondly, I am grateful to Dr.A. Haji Sheikh who taught me the required concepts through his course and for his valuable suggestions in the area of heat transfer. He is one of those professors who always maintained an ever-standing open door policy to guide students on their tasks in hand by his kind support. I am also grateful to Dr. Donald Wilson for his constant help and support whenever required. In spite of being busy, he is always there for the group meetings by providing academic support as well as ambition to explore new ideas and concepts.

Lastly and most important, I cannot end without thanking my father Krishnam Raju, mother Varalakshmi, brother Phani Kishore and fiancé Mohan Raju on whose constant love and encouragement I have relied all through my academic life. I am also thankful to all my friends from University of Texas at Arlington for being the surrogate family during the two years and for their continued moral support.

November 23, 2009

ABSTRACT

HEAT TRANSFER ANALYSIS OF

A PULSE DETONATION

ENGINE

NEELIMA KALIDINDI, MS

The University of Texas at Arlington, 2009

Supervising Professor: Dr. Frank Lu

A thermal analysis of the effect of sensible heat release on the walls of the detonation chamber for stoichiometric mixtures of hydrogen/air, octane/air and octane/oxygen was presented. The detonation tube was assumed to operate at 20 Hz and cooled by a water jacket to dissipate the heat from the walls which ensures the effective operation for a longer period. Wall material was assumed to be made of copper because of its high thermal conductivity.

The study showed a slow temperature rise along the walls of the combustion chamber for multiple pulses. It can be concluded that due to the space-time averaging procedure throughout the length of the tube, the temperature rise along the inner and outer walls are small. Even after 3000 pulses, the temperatures along the surfaces were almost steady.

TABLE OF CONTENTS

LIST OF ILLUSTRATIONS

Figure Page

LIST OF TABLES

NOMENCLATURE

a	Sonic speed of gas
A	Circumferential area of the detonation tube
$\mathrm{C_p}$	Specific heat at constant pressure
$\mathrm{C_v}$	Specific heat at constant volume
CEA	Chemical Equilibrium with Applications (code)
$\mathrm{D_{CJ}}$	Speed of Chapman-Jouguet detonation wave
f	Frequency
$\mathrm{F(r^1)}$	Initial temperature distribution equation at location $\mathrm{r^1}$
$\mathrm{g(r^1, \tau)}$	Volumetric energy equation at location $\mathrm{r^1}$ and time τ
G	Green's function
∇h	Change in enthalpy
H	Overall heat transfer coefficient
K	Thermal conductivity
L	Length of the pulse detonation engine
M	Mass flow rate of the gas
$\mathrm{M_{CJ}}$	Chapman-Jouguet detonation Mach number
np	Number of cycles
p	Pressure
PDE	Pulse detonation engine
Q	Heat flux

$\dot{Q}$	Heat release during one cycle
r_i	Inner radius of the detonation tube
r_o	Outer radius of the detonation tube
R	Gas constant
T	Time
t_1	Time of rarefaction wave
t_{fill}	Time taken during filling process
t_{pur}	Time taken during purging process
t_{rar}	Time taken during rarefaction process
t_{cj}	Time taken during detonation process
t_{exh}	Time taken during exhaust process
t_{cyc}	Period of cyclic pulse detonation engine operation
T	Temperature
TW_1	Temperature of the inner wall of the detonation tube
TW_2	Temperature of the outer wall of detonation tube
T_∞	Ambient temperature
τ	Time due to pulse of heat
v, u	Velocity of the gas flow
V	Volume of the detonation tube
X	Reference location inside the detonation tube
x_2	Axial distance from the closed end
Γ	Gamma
P	Density
A	Thermal expansion coefficient

Subscripts

e	Exit of heat exchanger
ex	Open-end boundary of rarefaction wave originating from open end
i	Inlet of heat exchanger
1	Undisturbed state of the detonable mixture
2	Chapman-Jouguet state
3	Rear boundary of rarefaction wave
∞	Ambient surroundings

CHAPTER 1

INTRODUCTION

1.1 Pulse Detonation Engine

The potential advantages of pulse detonation engines (PDEs) over conventional deflagration-based engines have been investigated for many years. Copious publications have appeared describing the potential for this type of propulsive device. Pulse detonation engine offer a low - cost alternative to existing engines due to their high thermodynamic cycle efficiency, lack of moving parts, high thrust-to-weight ratio, simple structure, operational range, low acquisition and maintenance cost. Hence it is expected to be a high performance, future generation aerospace propulsion engine.

System studies of PDEs as is common in the study of energy conversion processes use a quasi-one-dimensional approach. For simplicity in this study, the PDE is assumed to be a straight tube with constant cross section in which one end of the tube is closed and other end is open. A detonation wave is ignited at the closed end. It is usual to assume that the flow is independent of viscous effects and thermal conduction.

A detonation wave is simply described as one-dimensional structure consisting of a leading shock wave followed by a coupled reaction zone which propagates at a steady velocity termed as the Chapman-Jouguet (CJ) detonation velocity, which depends on the mixture initial parameters like temperature, pressure and energy content. In PDEs, the ignition of the fuel has been given much attention since it involves difficulties in rapidly mixing the fuel and oxidizer at high speeds and initiating, maintaining the detonation in a controlled manner.

Though most researchers have been concentrating on the detonation process, not much attention has been given to thermal management. One of the important challenges of pulse detonation engines is that the detonation chamber walls get heated by the combustion products to a temperature much greater than the temperature of self-ignition arising from the rapid pulsed energy release from detonation in fractions of a millisecond. Hence the engine needs to be cooled to prevent auto-ignition. In addition, the high temperature may cause catastrophic failure.

In this present study, the interest is on the heat transfer that arises from the detonation. For this, we consider the pulse detonation engine to be a tube of 1 m long with 100 mm bore, operating at 20 Hz with stoichiometric mixtures of hydrogen/air, octane/air and octane/oxygen.

1.2 Operating Principle of Pulse Detonation Engine

In pulse detonation engines, when the reactive mixture is ignited at the closed end, the pressure in the chamber increases due to the propagation of a detonation wave that consists of a shock wave coupled with a flame front. The shock wave acts as a virtual piston between detonation products and fresh mixture. The velocity of the "virtual detonation piston" is higher than the velocity of conventional combustion being in the order of 1000-5000 m/s.

As highlighted above, the pulse detonation engines uses the energy released from repeated detonations in a cyclic mechanism. Each cycle can be divided into six processes namely filling, Chapman-Jouguet detonation, Taylor rarefaction, reflected rarefaction, exhaust and purging as shown in Figure 1.1[1] which are clearly explained in the following sections.

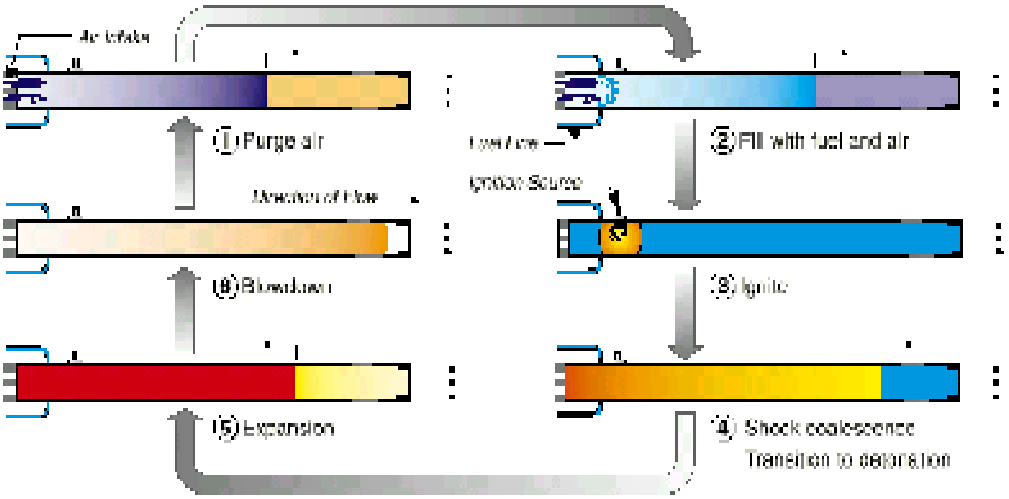

Figure1.1. Schematic of PDE showing various stages during one cycle[1]

1.2.1 Filling Process

This first stage in a PDE operation is to fill the tube with a detonable mixture of fuel and oxidizer. The injection of fuel and oxidizer into the combustion chamber can be characterized by a frequency of $f = 1/t_{cyc}$. In general the frequency depends on various parameters like length and diameter of the combustion chamber, injection pressure, and the types of ratios of fuel and oxidizer. This fill process from the closed end occurs at a very low speed of 20-30m/s. The filling time plays an important role in the PDE cycle since it affects the timing of all other processes. If there is delay in filling the detonation process will be delayed.

1.2.2 CJ Detonation Process

This is the second stage where the mixture is ignited and the detonation wave moves from the closed end to the open end with very high velocities termed as the Chapman-Jouguet (CJ) velocity of 1000- 5000m/s in fractions of a millisecond leaving behind high temperatures and pressures .The high enthalpy from the detonation wave produces thrust when the exhaust gases are allowed to exhaust through a nozzle. The

time for the propagation of a detonation wave is very short when compared to any other process due to the very high wave speeds.

1.2.3 Taylor Rarefaction Process

While the detonation wave propagates towards the open end, the gas between the closed end which is at rest and detonation wave is decelerated. This decelerated gas requires the generation of an unsteady expansion known as the Taylor rarefaction wave which propagates behind the detonation wave. Hence the front boundary condition of Taylor rarefaction coincides with detonation wave while rear boundary of the Taylor rarefaction matches that of the closed end. The time taken for the Taylor rarefaction process is higher than detonation since it travels at velocities lower than the detonation wave.

1.2.4 Reflected Rarefaction Process

This is the fourth stage in which another set of rarefaction waves starts propagating from the open end which travels at sonic velocity and reaches the closed end. This reflected rarefaction wave drops the pressure to a lower value due to expansion of waves.

1.2.5 Exhaust Process

When the unsteady reflected rarefaction starts propagating towards the closed end, it scavenges the burned gas, exhausting it from the open end and clearing the tube from unwanted reactive impurities. This results in a cool, empty chamber that is ready to be filled.

1.2.6 Purging Process

This is the last stage in which the tube is recharged with a fresh air mixture and the pressure is assumed to decay linearly until it reaches ambient conditions. This process plays a vital role in cleaning the impurities inside the detonation tube with the fresh air pumped at high velocities without which may lead to auto-ignition of the mixture

and ultimately leads to destruction of the combustion walls. The time taken for filling and purging are almost the same.

The total time for one cycle is thus given by

$$t_{cyc} = t_{fill} + t_{cj} + t_{rar} + t_{exh} + t_{pur} \quad [1]$$

1.3 Objective of the Current Research

One of the challenges in developing a PDE is the high post-detonation gas temperatures produced in the range of 1700- 3000 K. To minimize the heat loads on the combustion-chamber walls, a water jacket heat exchanger is proposed which ensures effective operation for a longer duration. Hence the objective of the current research is to perform a thermal analysis through the walls of the combustion chamber and develop a cooling technique.

1.4 Heating Analysis

1.4.1 Energy Equation

The heat generated during various processes of the intermittent engine can be computed in many ways. We consider the energy equation in which each process of the pulse detonation engine is separately considered as a control volume and the heat developed is calculated using the equation below.

$$q = c_p T + \frac{v^2}{2} \quad [2]$$

After calculating the heat developed in each processes, the wall temperatures of the detonation tube (TW_1 and TW_2) are calculated using a Green's function approach. This approach assumes a hollow concentric cylinder with the detonation process occurring in the inner cylinder and water as a coolant is assumed to flow in the concentric cylinder. The detonation tube has an inner and an outer radius of r_i (TW_1) and r_0 (TW_2) respectively. The heat transfer analysis can also be estimated at various locations through the diameter of the tube by varying the inner and outer radius for any number of cycles.

The present research is to develop an understanding of the heating of the combustion chamber affected by the heating and cooling pulses in multiple cycles during various processes for the three stoichiometric mixtures of hydrogen/air, octane/air and octane/oxygen. This study also recommends materials which can sustain the heat loads.

CHAPTER 2

THERMODYNAMIC CALCULATIONS

This chapter discusses the procedure to determine the heat release during one PDE cyclic for stoichiometric mixtures of hydrogen/air, octane/air and octane/oxygen.

Properties like temperature, pressure and density during detonation, Taylor rarefaction, reflected rarefaction and exhaust are considered and discussed. The heating rates for these processes are very high when compared with those in the filling and purging processes which allow them to be neglected. The front and rear boundary conditions of the considered processes are explained and average conditions are evaluated.

2.1 Prior Research

Though most researchers are focusing on the performance of the PDEs by considering various parameters for producing reliable detonations, the experiments conducted by Hoke et al.[2] gives a practical solution to thermal management. Their experiments obtained the overall heat load for stoichiometric mixture of hydrogen/air. They measured heating rates for a 0.91 m detonation tube with a 50 mm bore surrounded by a water-cooled, annular aluminum jacket with an outer diameter of 63.4 mm. The overall heat load was measured calorimetrically, while the wall temperatures were measured separately using thermocouples spot welded to the detonation tube. Hoke at al.[2] found heating rates of 21 KW for detonations at 20 Hz. Considering this heat rate during the cyclic process, an average heat flux of q=1.7 $\mathrm{MW/m^2}$ is obtained. In addition when the frequency is doubled from 20 to 40 Hz it was found that the heat load

increases only by 58%. The equivalence ratio and cycle frequency were found to have the largest impact on the detonation tube heat loads. Ajmani and Breisacher[3] observed for the same mixture a different time-averaged heat flux value of 2.5 $\mathrm{MW/m^2}$. But the latter measurements were time averaged at a single location of the tube, where as the results of Hoke at al.[2] were time and space averaged throughout the length of the tube. Experimental observations[4] were carried for detonation of a stoichiometric mixture of JP-10 vapor and air to study the detonation properties for a 6.2 m long, 10 cm inner diameter heated detonation tube at initial mixture pressure of 2 atm and initial temperatures of 373, 473 and 528 K. Besides experimental observations, thermodynamic cycle analyses have been performed at high detonation temperatures by considering the sensible heat release on the pulse detonation engine parameters[5]. Preliminary heat exchanger design[6] for a 1 m long and 100 mm bore, operated at 19 Hz was performed for stoichiometric octane/air. Results showed the detonation wall temperatures to be between 1000- 1200 K for materials like stainless steel, copper and Haynes alloy (H282) for multiple cycles.

2.2 Properties of CJ Detonation Wave

Based on the simplified analysis of a pulse detonation engine model by Endo and Fujiwara[7,8] the properties of detonation, rarefaction and exhaust are calculated.

As discussed, ignition of the mixture leads to the generation of a detonation wave which travels at the Chapman-Jouguet velocity towards the open end. For this study, it is assumed that detonation occurs instantaneously, that is, the so-called deflagration-to-detonation transition does not occur. The properties downstream of the detonation wave are characterized by ρ_2, p_2 and T_2 as shown in Figure 2.1.

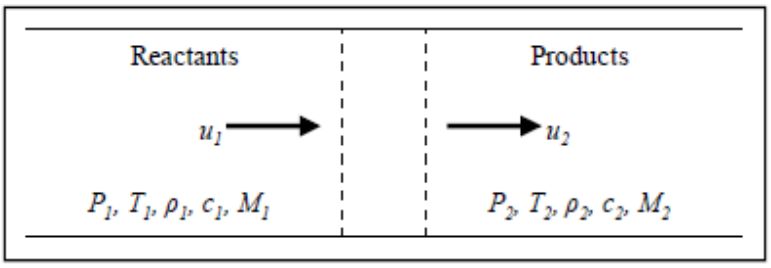

Figure 2.1. Flame propagation from left to right

The time taken for the detonation wave to propagate through the 1 m tube for the three stoichiometric mixtures varies because of the different values of the Chapman-Jouguet velocities. The equation given below is used to evaluate the propagation time. The results for the three cases are given in table 2.1

$$t = \frac{\text{length of the tube}}{\text{detonation velocity}} \quad [3]$$

Table 2.1 Detonation Wave Propagation Time

	Hydrogen/Air	Octane/Air	Octane/Oxygen
Detonation time, s	0.0005	0.00055	0.00043

When the heat release during chemical reaction is much higher than the internal energy of the unburned gases the detonation properties can be calculated by using the Rankine-Hugoniot relations[7,8] which are given by

$$\rho_2 = \frac{\gamma_2+1}{\gamma_2}\rho_1 \quad [4]$$

$$P_2 = \frac{\gamma_1}{\gamma_2+1} M_{CJ}{}^2 P_1 \quad [5]$$

$$D_2 = D_{CJ} = \sqrt{2(\gamma_2{}^2 - 1)q} \quad [6]$$

$$u_2 = \frac{1}{\gamma_2}\, a_2 = \frac{1}{\gamma_2+1} D_{CJ} \quad [7]$$

Tables 2.2–2.4 show the calculated detonation values (State 2) using the above relations[7,8] where the (State 1) values are the initial conditions.

Table 2.2 Detonation Properties of Stoichiometric Hydrogen and Air

Parameters	State 1	State 2
$\rho,\ kg/m^3$	1.168	1.529
p, atm	1	15.38
T,K	300	2954
γ	1.4015	1.636
$C_p,\ J/kg\ K$		3.3615
$C_v,\ J/kg\ K$		0.5728
M_{CJ}		4.8315
$R,\ J/kg.K$		345

Table 2.3 Detonation Properties of Stoichiometric Octane and Air

Parameters	State 1	State 2
$\rho, kg/m^3$	1.168	2.23
p, atm	1	18.39
T, K	300	2904
γ	1.3483	1.1649
$C_p,\ J/kg\ K$		2.7368
$C_v,\ J/kg\ K$		0.4851
M_{CJ}		5.4019
$R,\ J/kg.K$		287

Table 2.4 Detonation Properties of Stoichiometric Octane and Oxygen

Parameters	State 1	State 2
$\rho,\ kg/m^3$	1.168	2.19
p, atm	1	38.82
T,K	300	3831
γ	1.2365	1.1378
$C_p,\ J/kg\ K$		8.6742
$C_v,\ J/kg\ K$		1.7066
M_{CJ}		8.0438
$R,\ J/kg.K$		352

2.3 Average Conditions during Detonation Process

The state of the gas downstream of the detonation wave is given by the relations of self-similar rarefaction wave[7,8] since the front boundary conditions of this wave coincide with the detonation wave and the state of the gas are given by p_2, T_2, ρ_2. Hence the average detonation conditions are calculated by using these relations as

$$\rho = \left(\frac{1}{\gamma_2} + \frac{\gamma_2-1}{\gamma_2}\frac{x}{x_2}\right)^{\frac{2}{\gamma_2-1}} \rho_2 \quad [8]$$

$$p = \left(\frac{1}{\gamma_2} + \frac{\gamma_2-1}{\gamma_2}\frac{x}{x_2}\right)^{\frac{2\gamma_2}{\gamma_2-1}} p_2 \quad [9]$$

$$u = u_2 - \frac{2}{\gamma_2+1}\frac{x_2-x}{t} = -a + \frac{x}{t}\left(\leq \frac{1}{\gamma_2}a\right) \quad [10]$$

$$a = a_2 - \frac{\gamma_2-1}{\gamma_2+1}\frac{x_2-x}{t} \quad [11]$$

The length of the tube, x_2 =1 m. The average temperature, pressure and density are calculated by varying the position of the detonation wave x, throughout the length of the tube.

Figures 2.2 and 2.3 show the properties of detonation wave at any location of the tube for the three stoichiometric mixtures. It can be noted that octane/oxygen has the highest properties because of higher velocity and Mach number.

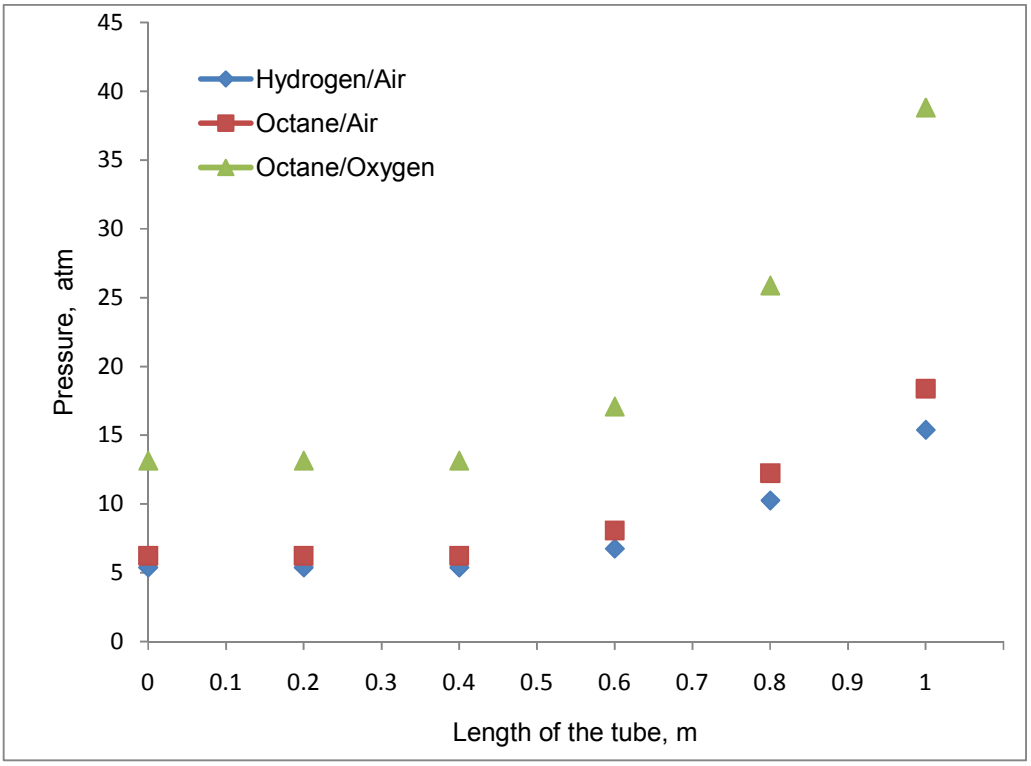

Figure 2.2. Pressure distribution of detonation wave for three stoichiometric mixtures along the length of the tube

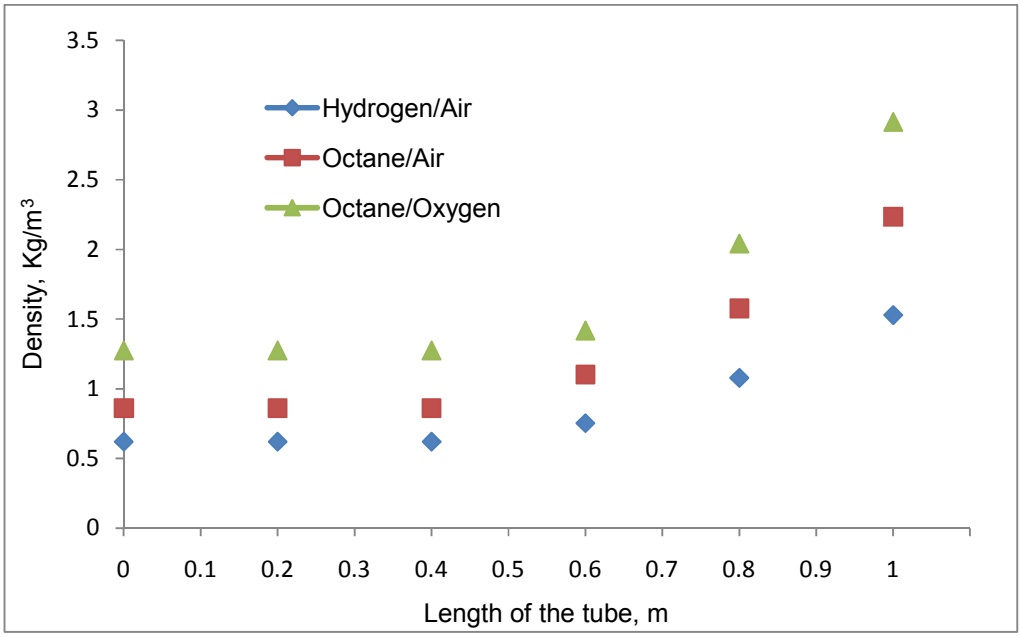

(a)

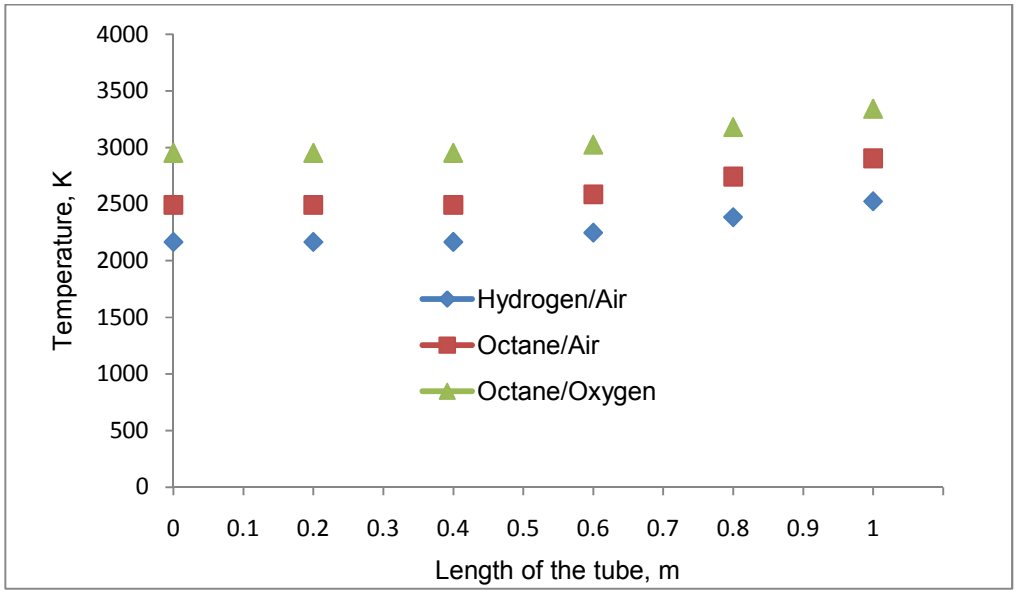

(b)

Figure 2.3. Properties of detonation wave for three stoichiometric mixtures along the length of the tube (a) density and (b) temperature

2.4 Boundary Conditions of Rarefaction Wave

Since the leading edge of the Taylor rarefaction wave follows immediately behind the detonation wave the properties of detonation becomes the front boundary conditions of the Taylor rarefaction. The state of the gas at the rear boundary of the rarefaction wave is given as follows

$$x_3 = \frac{1}{2}x_2 \quad [12]$$

$$D_3 = a_3 = \frac{1}{2}D_{CJ} \quad [13]$$

$$\rho_3 = 2\left(\frac{\gamma_2+1}{2\gamma_2}\right)^{\frac{\gamma_2+1}{\gamma_2-1}}\rho_1 \quad [14]$$

$$p_3 = \frac{\gamma_1}{2\gamma_2}\left(\frac{\gamma_2+1}{2\gamma_2}\right)^{\frac{\gamma_2+1}{\gamma_2-1}}{M_{CJ}}^2 p_1 \quad [15]$$

Using the above relations the rear conditions of rarefaction wave (State 3) are evaluated and displayed in Tables 2.5 – 2.7

Table 2.5 Rarefaction Properties of Hydrogen/Air

Parameters	State 1	State 3
$\rho,\ \mathrm{kg/m^3}$	1.168	0.891
p, atm	1	5.36
T, K	300	1290
γ	1.4015	

Table 2.6 Rarefaction Properties of Octane /Air

Parameters	State 1	State 3
$\rho,\ \mathrm{kg/m^3}$	1.168	0.891
p, atm	1	4.55
T, K	300	1335
γ	1.3483	

Table 2.7 Rarefaction Properties of Octane/Oxygen

Parameters	State 1	State 3
$\rho,\ \mathrm{kg/m^3}$	1.168	0.886
$\mathrm{p, atm}$	1	13.33
T, K	300	1451
γ	1.2365	

2.5 Average Conditions during Unsteady Rarefaction Process

As the detonation wave leaves the tube, another unsteady rarefaction expansion starts propagating in the opposite direction where the products are exhausted from the open end through this unsteady rarefaction. Hence the front boundary conditions of this reflected wave are the rear conditions of the Taylor rarefaction wave. The state of the flow inside the tube is given by the self-similar rarefaction wave[7,8] as

$$\rho = \left(1 + \frac{\gamma_2 - 1}{D_{CJ}} \frac{L - x}{t - t_1}\right)^{\frac{2}{\gamma_2 - 1}} \rho_{ex} \qquad [16]$$

$$p = x\left(1 + \frac{\gamma_2 - 1}{D_{CJ}} \frac{L - x}{t - t_1}\right)^{\frac{2\gamma_2}{\gamma_2 - 1}} \qquad [17]$$

$$a = a_{ex} + \frac{\gamma_2 - 1}{\gamma_2 + 1} \frac{L - x}{t - t_1} \qquad [18]$$

where

$$\rho_{ex} = \frac{\gamma_2 + 1}{\gamma_2^{\frac{\gamma_2 + 1}{\gamma_2 - 1}}} \rho_1 \qquad [19]$$

$$p_{ex} = \frac{\gamma_1}{\gamma_2^{\frac{2\gamma_2}{\gamma_2 - 1}} (\gamma_2 + 1)} M_{CJ}{}^2 p_1 \qquad [20]$$

$$u_{ex} = a_{ex} = \frac{1}{\gamma_2 + 1} D_{CJ} \qquad [21]$$

The final conditions are given by the exit conditions of the gas by self-similar rarefaction wave[7,8] which are displayed in Tables 2.8 – 2.10.

Table 2.8 Exit Conditions for Rarefaction Wave of Hydrogen/Air

Parameters	State 1	Exit State
$\rho,\ \mathrm{kg/m^3}$	1.184	0.341
$\mathrm{p, atm}$	1	1.73
T,K	300	1088
γ	1.4015	

Table 2.9 Exit Conditions for Rarefaction Wave of Octane /Air

Parameters	State 1	Exit State
$\rho,\ \mathrm{kg/m^3}$	1.184	0.341
$\mathrm{p, atm}$	1	2.08
T,K	300	1592
γ	1.3483	

Table 2.10 Exit Conditions for Rarefaction Wave of Octane/Oxygen

Parameters	State 1	Exit State
$\rho,\ \mathrm{kg/m^3}$	1.31	0.337
$\mathrm{p, atm}$	1	4.38
T,K	300	1254
γ	1.2365	

For calculating the average properties during rarefaction process using the equations [16] and [17] the following are the considerations. The rarefaction time, $t =$

0.00345 s, 0.00358 s, 0.00353 s for hydrogen/air, octane/air, octane/oxygen respectively. The coordinate x and time t_1 are varied. Time t_1 is varied between detonation and rarefaction phase since the rarefaction starts after detonation till the time t. The average pressure, density and temperature are calculated by varying the position of the rarefaction wave x, throughout the tube at different times t_1.

The histories of temperature, pressure and density for hydrogen/air are shown at times $t_1 = 0.001\ \text{s}, 0.002\ \text{s and } 0.00353\ \text{s}$. In Figures 2.4 and 2.5 it can be noted that the decay of these properties at the start of rarefaction wave is rapid and becomes slow towards the exit of the tube.

2.5.1 Comparison of Unsteady Rarefaction Properties of Hydrogen/Air, Octane/Air and Octane/Oxygen

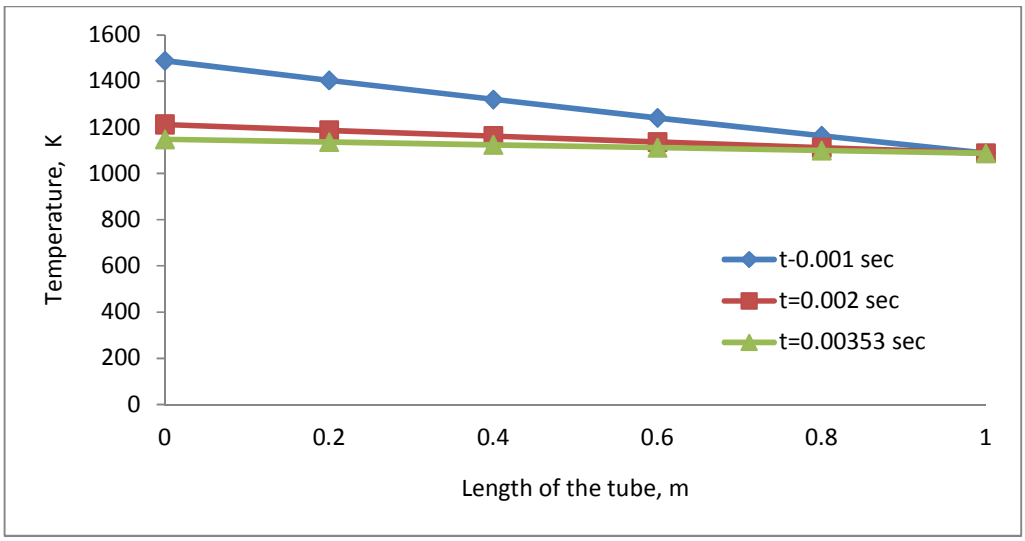

Figure 2.4. Temperature distribution at various times of unsteady rarefaction wave for hydrogen/air till the exit of the tube

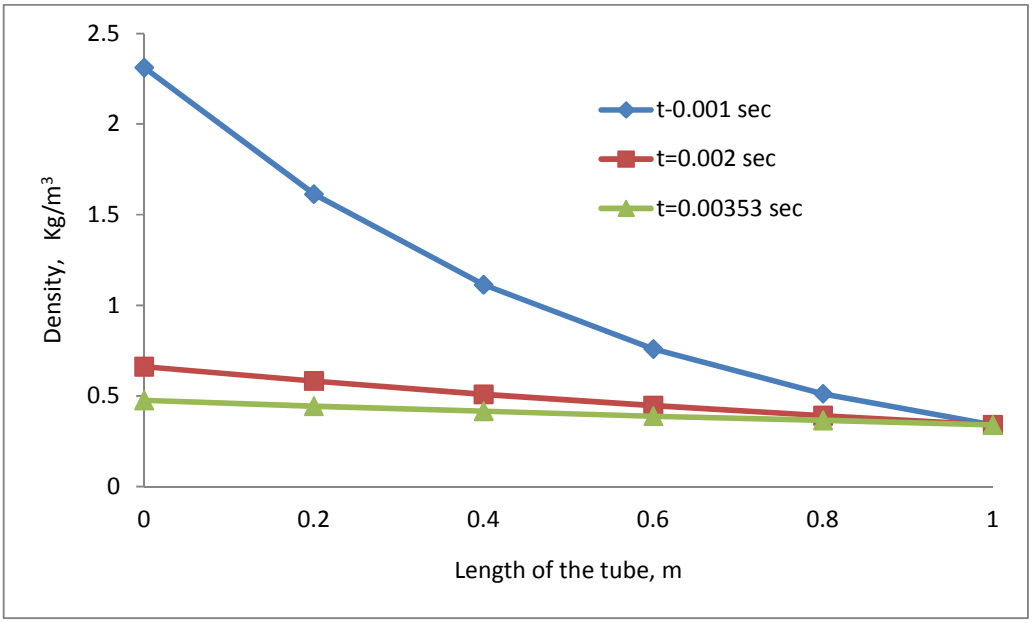

(a)

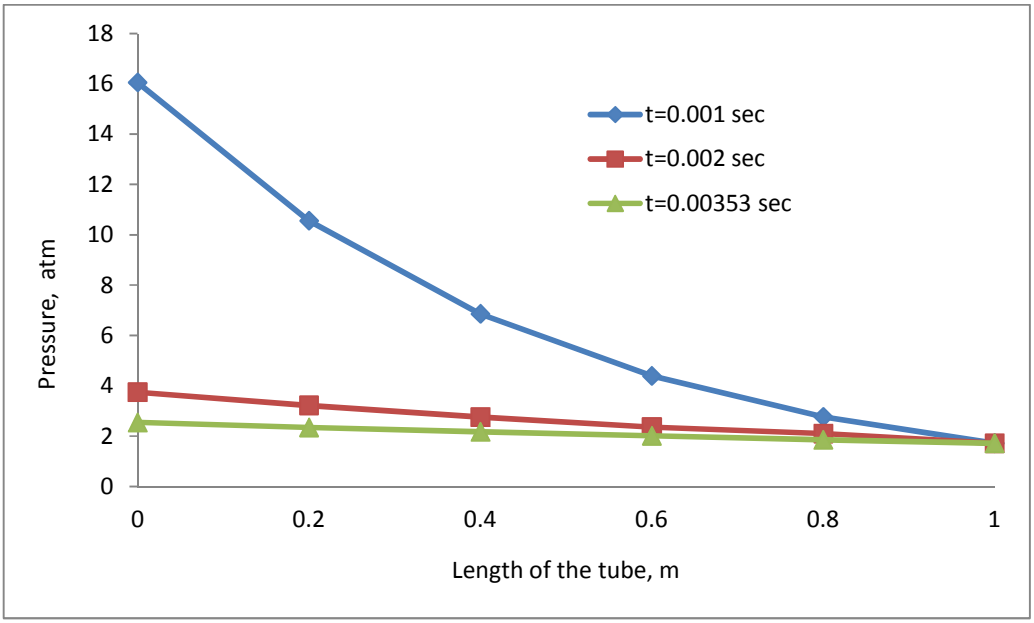

(b)

Figure 2.5. Properties of unsteady rarefaction wave for hydrogen/air till the exit of the tube (a) density at various times (b) pressure at various times

Figures 2.6 and 2.7 compare the temperature in the reflected unsteady rarefaction at various times for the three stoichiometric mixtures. It can be noted that the temperature does not decay much for the octane/air mixture when compared with other mixtures though octane/oxygen mixture has a higher detonation temperature. It can be estimated that the temperature of octane/oxygen decayed faster because of its higher gas constant.

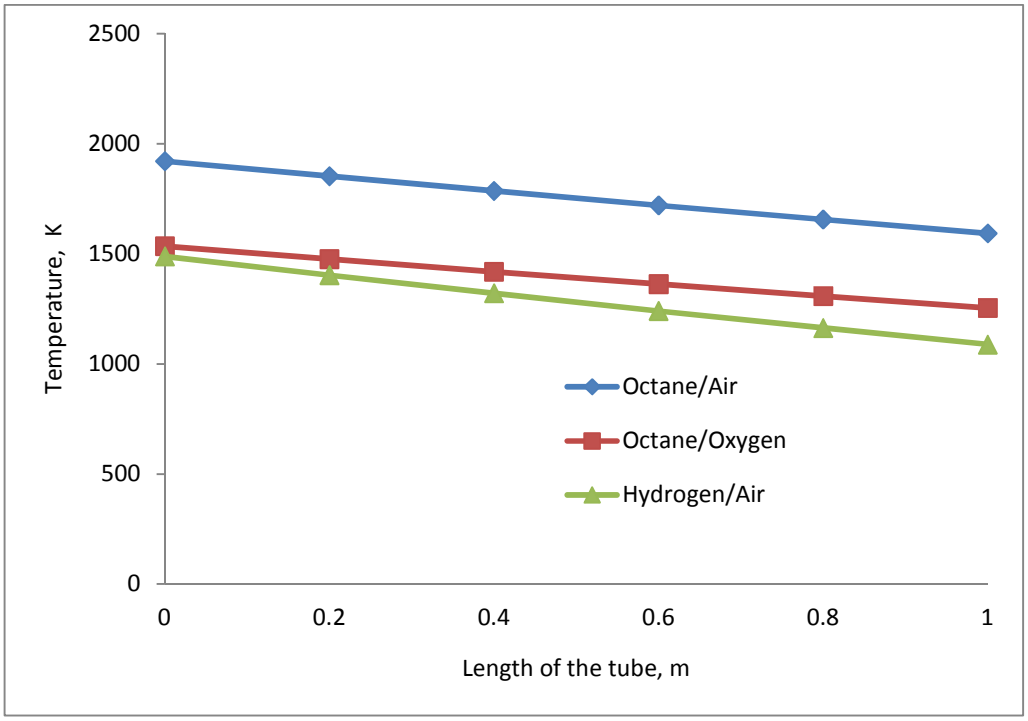

Figure 2.6. Comparison of temperature profiles of unsteady reflected rarefaction wave for the three stoichiometric mixtures at, t= 0.001 sec

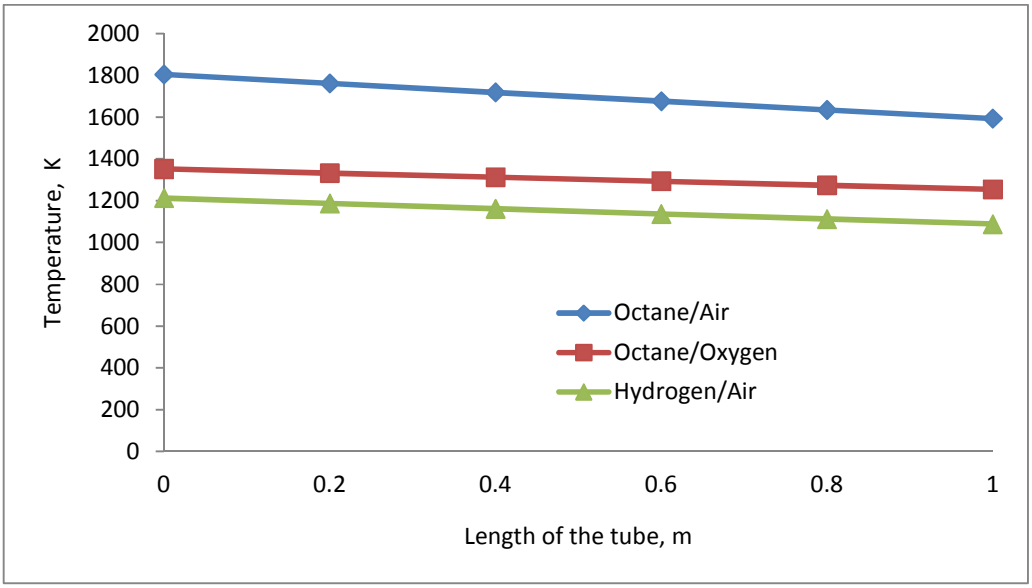

(a)

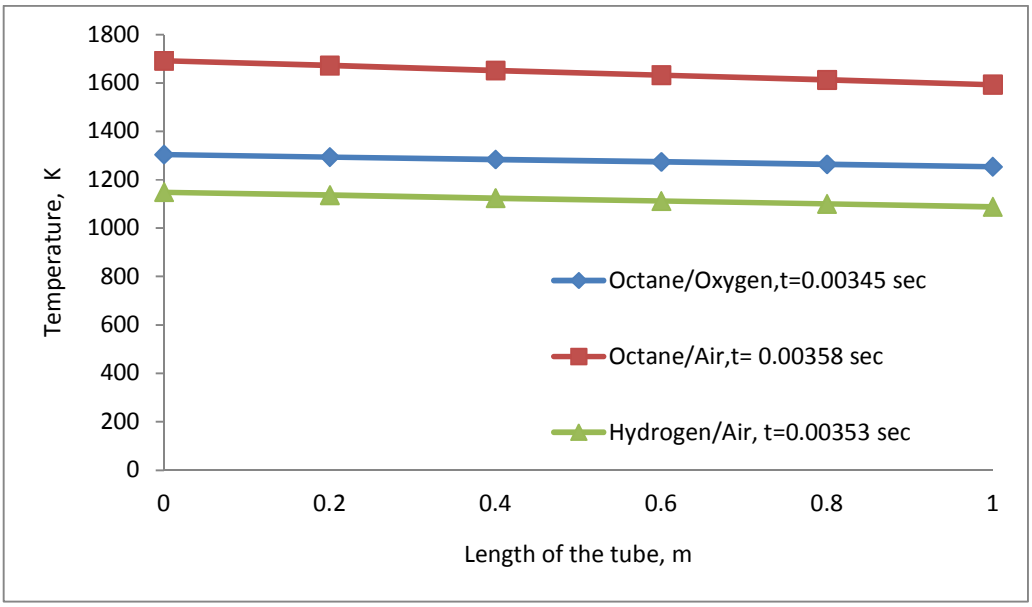

(b)

Figure 2.7. Comparison of temperature profiles of unsteady reflected rarefaction wave for the three stoichiometric mixtures at various times (a) temperature profile at, t= 0.002 sec and (b) temperature profile at the exit of the wave

Figures 2.8 and 2.9 show the comparison of pressure and density at various times for the three stoichiometric mixtures. It can be noted that octane/oxygen yielded the highest pressure and density. Decay of these properties is rapid at the start of the rarefaction wave for all the three mixtures.

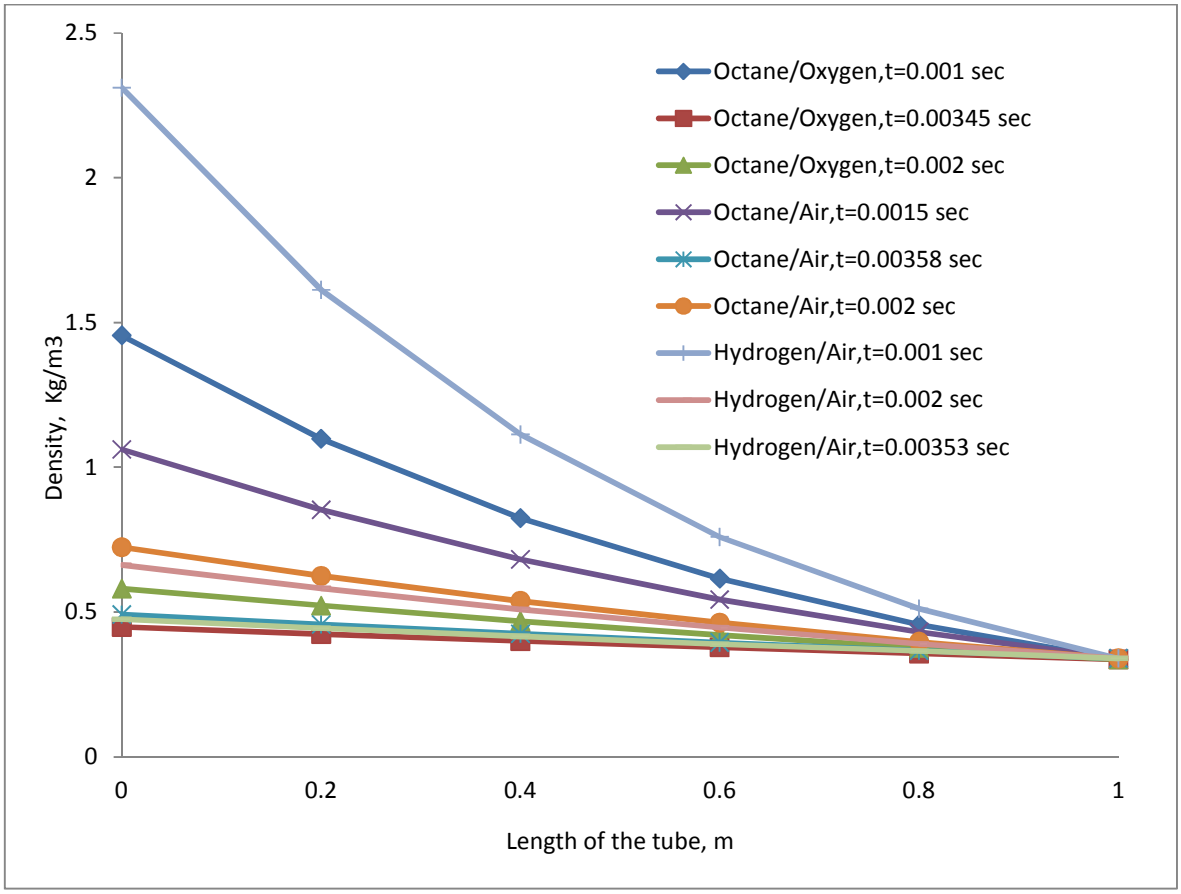

Figure 2.8. Comparison of density's at various times for three stoichiometric mixtures

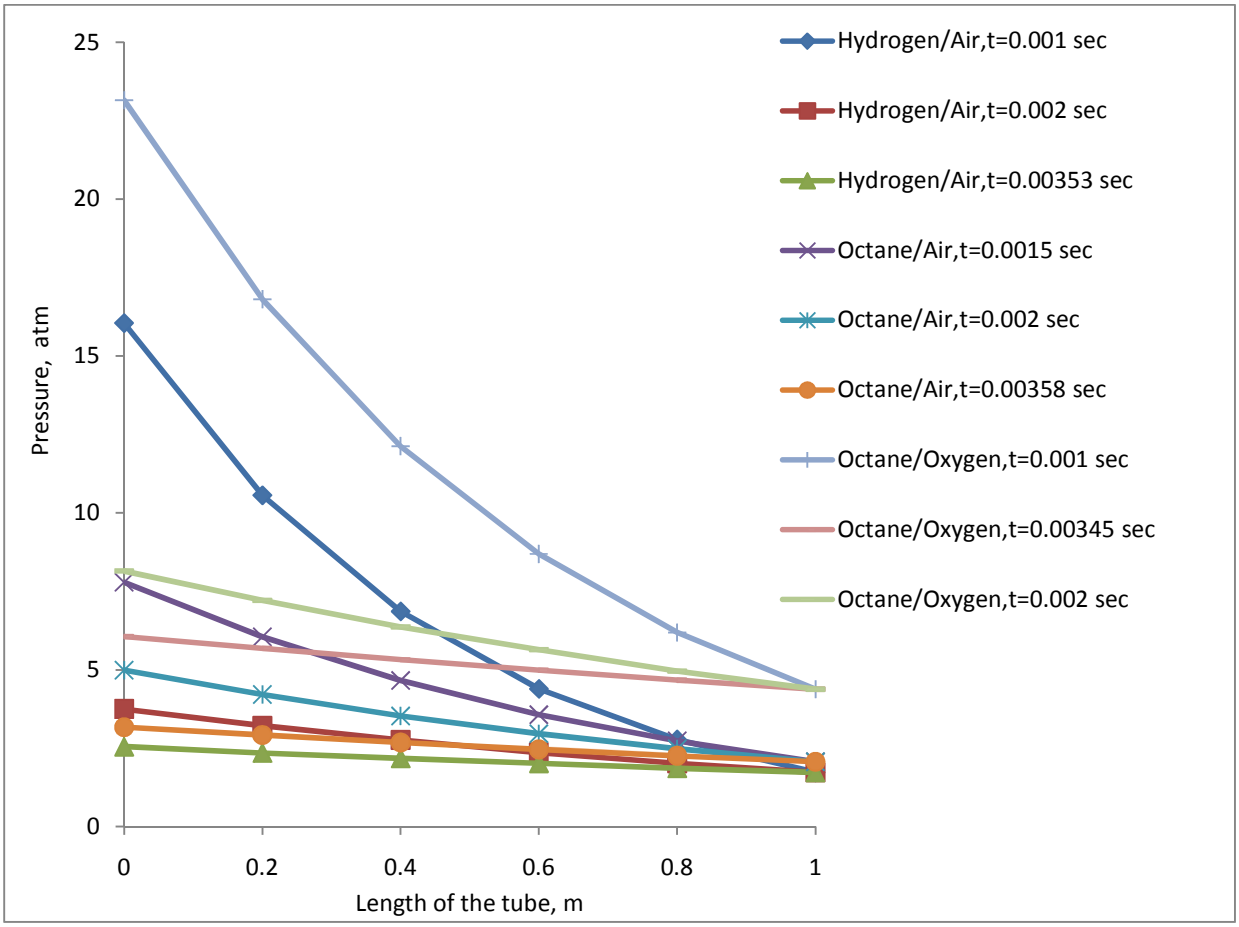

Figure 2.9. Comparison of pressure's at various times for three stoichiometric mixtures

2.6 Calculation of Heat Generation for One Cycle of Operation

Figure 2.10 shows a control volume open system, which is an application of first law of thermodynamics[9]. It is a widely used concept in the thermodynamic analysis of many types of equipment. Therefore the heat release can be calculated by steady-flow energy equation[9]

$$\dot{m}(\Delta h) = \dot{Q} \qquad [22]$$

$$\dot{m}\left(c_p dT + \frac{v^2}{2}\right) = \dot{Q} \qquad [23]$$

where $\dot{Q}[W]$ is the rate of heat transfer, $\dot{m}[kg/s]$ is the mass flow rate, $v[m/s]$ is the velocity, $c_p[J/kg\,K]$ is the constant pressure specific heat.

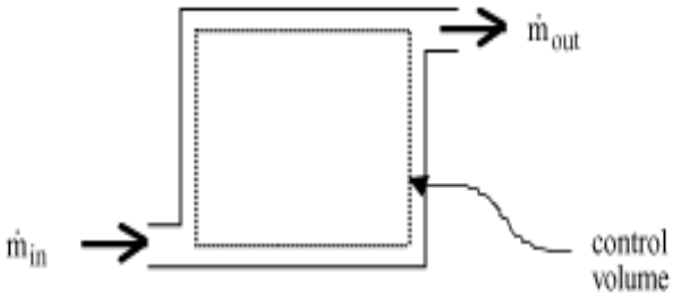

Figure 2.10. Application of energy conservation principle to a steady flow open system[9]

Considering inlet and exit conditions, the total heat release can be calculated from

$$\dot{Q} = m_e\left(c_p T_e + \frac{v_e^2}{2}\right) - m_i\left(c_p T_i + \frac{v_i^2}{2}\right) \quad [24]$$

The inlet conditions are at STP but the exit conditions are the average values of detonation and rarefaction process.

Table 2.11 Inlet and Exit Enthalpy Calculations

		t, s	$\dot{m}$, kg/s	v, m/s	c_pT	mh, kJ
Inlet Conditions		0.02	0.48	50	300	14.9
Exit Conditions	Hydrogen/Air	0.00353	1.45	201	2856	118.5
	Octane/Air	0.00358	1.67	250	3500	207.63
	Octane/Oxygen	0.00345	2.13	296	3820	344.37

Table 2.12 Total Heat Generated for the Three Stoichiometric Mixtures

	Hydrogen/Air	Octane/Air	Octane/Oxygen
Heat Release $\dot{Q}$, MJ	0.1037	0.1927	0.3295

CHAPTER 3

DETERMINATION OF DETONATION WALL TEMPERATURES

3.1 Introduction

As the PDE uses the energy released from repeated detonations, the tube gets heated to very high temperatures. For thermal management, the detonation tube is assumed to be surrounded by water which acts as a coolant at STP conditions. The flow in the detonation tube of constant cross section is assumed to be one dimensional.

For the simplified analysis, the detonation tube is assumed to be a hollow concentric cylinder with inner surface of radius [r_i] = 0.05 m and outer surface of radius [r_0] = 0.07 m. The outer surface of the tube is cooled by the coolant as shown in Figure 3.1. But the inner surface experiences various temperatures due to the different thermodynamic processes discussed in chapter 2. The temperatures along the inner and outer surfaces of the detonation tube are described as TW_1 and TW_2. The detonation tube is assumed to be made of copper since the thermal conductivity or ability to sustain high temperatures of this material is very high.

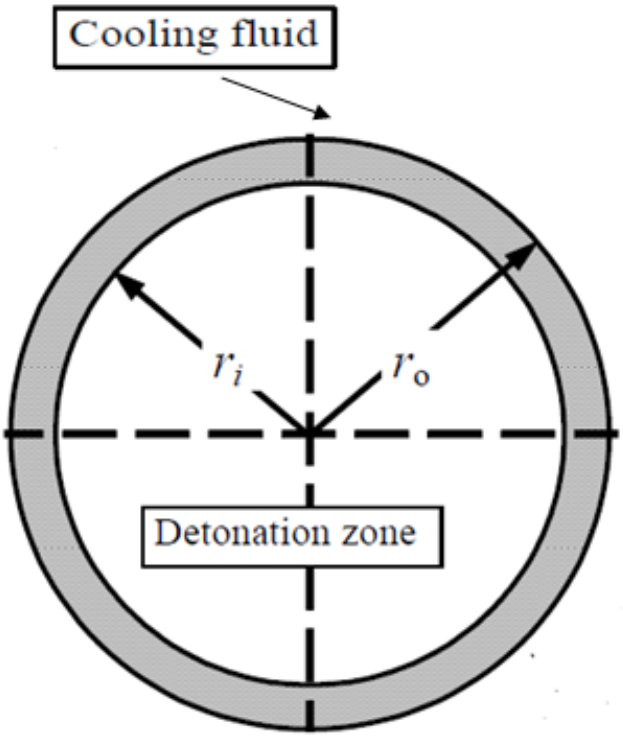

Figure 3.1 Cross sectional view of detonation tube

The effect of the cyclic mechanism of PDE for number of pulses on the walls of combustion chamber is discussed for the three stoichiometric mixtures by calculating the wall temperatures TW_1 and TW_2. Each cycle or pulse can be differentiated as heating and cooling pulse. The heating pulse is the period where the detonation wave propagates through the tube causing the tube temperature to rise. The cooling pulse is the period of the rest of the processes.

3.2 Fuel Type

Various hydrocarbon fuels have been investigated to surmise the sensible heat release during a detonation. Recent investigations[10] suggested that the single–

component hydrocarbon, tricyclodecane known as jet propellant 10 (JP-10) is currently considered the fuel of choice for PDEs. Experimental observation[11] suggested that JP-10 acts as an endothermic fuel, which means it acts as a coolant which ultimately helps in thermal management. Pre-vaporizing the fuel can enhance the initiation of the detonation in a fuel- air mixture for PDE applications. Hence the choice concerning the selection of the fuel-air mixture is essential for designing of the heat exchanger.

3.3 Transient Heat Analysis using Green's Function

Rapid changes in temperature take place across the inner surface due to conduction through the walls and convection due to the coolant. The temperature distribution along these surfaces can be obtained by a transient analysis solution of heat conduction through hollow cylinders. Hence the temperature expression using Green's function[12] for a finite body with homogeneous boundary condition for transient heat analysis is given by the following equation

$$\mathrm{T(r,t)} = 2\pi \int_{\mathrm{r^1=r_i}}^{\mathrm{r_0}} \mathrm{G(r,t/r^1,0)F(r^1)r^1dr^1} + \frac{2\pi\alpha}{\mathrm{k}} \int_{\tau=0}^{\mathrm{t}} \int_{\mathrm{r^1=r_i}}^{\mathrm{r_0}} \mathrm{G(r,t/r^1,\tau)g(r^1,\tau)r^1dr^1d\tau} \quad [25]$$

where the boundary conditions are

$$\frac{\partial \mathrm{G}}{\partial \mathrm{r}} = 0 \text{ at } \mathrm{r} = \mathrm{r_i}, \;\; \mathrm{k}\frac{\partial \mathrm{G}}{\partial \mathrm{r}} + \mathrm{hG} = 0 \;\; \text{at } \mathrm{r} = \mathrm{r_0} \quad [26]$$

The wall temperatures for both the heating and cooling pulses can be calculated using the above equation. Due to the intricacy of the calculations involved, the Green's expression[12] was coded in Mathematica™ which calculates the wall temperatures. The input to the Mathematica code are the heat flux $\mathrm{q[W/m^2]} = \mathrm{\dot{Q}/A}$ where $\mathrm{\dot{Q}\,[W]}$ is taken from [Table 2.12] and the circumferential area is taken as $\mathrm{A[m^2]} = 0.314$, inner$[r_i]$ and outer radius$[r_0]$, thermal conductivity of copper $\mathrm{K\,[W/m\,K]} = 400$, specific heat at constant pressure $\mathrm{c_p\,[J/kg\,K]} = 385$ and $\mathrm{h[W/m^2K]} = 2190$, over all heat transfer coefficient of the water which is constant since the velocity with which the water flows is kept constant through the annular chamber.

3.4 Calculation of Wall Temperatures TW_1 and TW_2

3.4.1 Hydrogen and Air

The input data to the Mathematica code in this case is

a) $q = \dot{Q}/A = 330255\ W/m^2$

b) $h = 2190\ W/m^2\,K$

c) $np =$ number of cycles

d) $t_p = 0.0005\ s$ [detonation time]

e) $t_{end} = 0.04403\ s$ [total cyclic time]

f) $r_i = 0.05\ m$

g) $r_0 = 0.07m$

The analysis is carried out for one cycle of PDE and the following graphs show how the temperatures vary along the inner and outer walls. The only difference between the inner surface TW_1 and outer surface TW_2 calculations is that r_i is replaced by r_0 in equation (25) when it is given as an input to Mathematica.

Figure 3.2(a) shows how the temperature along the inner wall rises for one detonation wave propagation. It can be noted that the inner wall gets heated to 300.3 K for a stoichiometric mixture of hydrogen/air. The temperature decays to 300K as shown in the Figure 3.2(b) along the inner surface during the cooling pulse. According to CJ-theory[7,8], due to expansion of waves during reflected rarefaction process the properties of gas decays along the length of the tube after the exit of the detonation wave and therefore the temperature comes down by the end of the cycle as shown in Figure 3.2(b). Figure 3.3 shows the temperature profile duing one complete cycle along the inner surface. It is obvious that the wall gets heated up during the detonation.

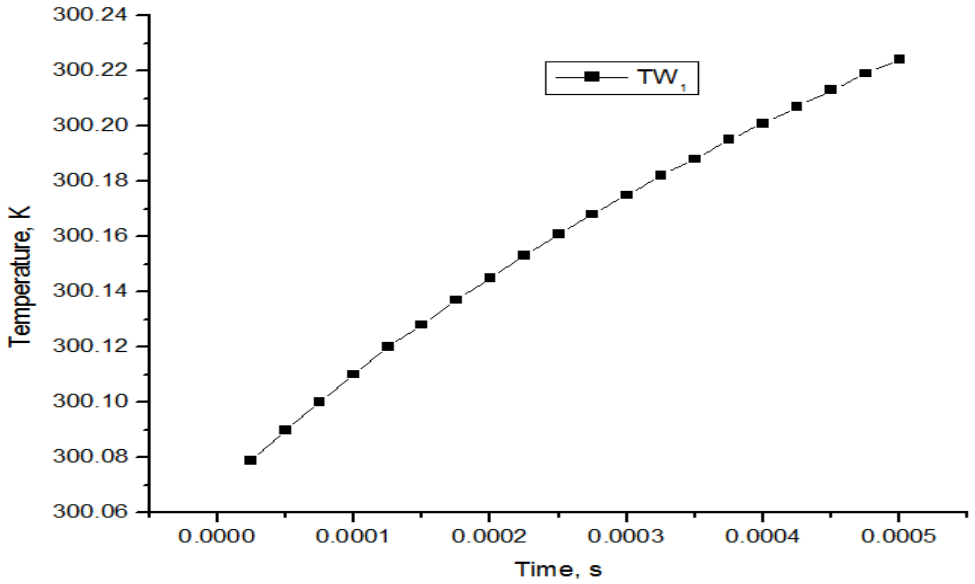

(a)

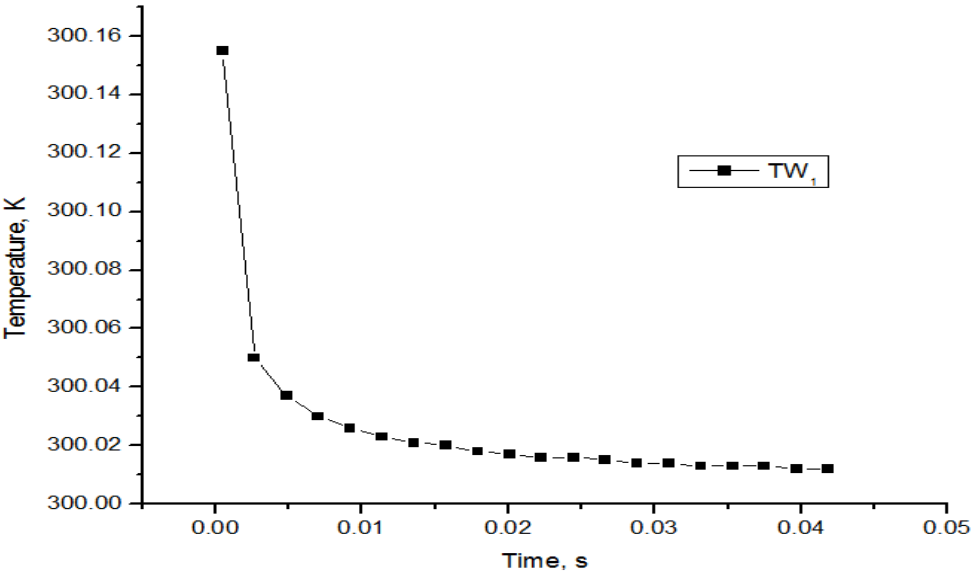

(b)

Figure 3.2. Variations in temperature along the inner wall (TW_1) for np=1 (a) heating pulse and (b) cooling pulse

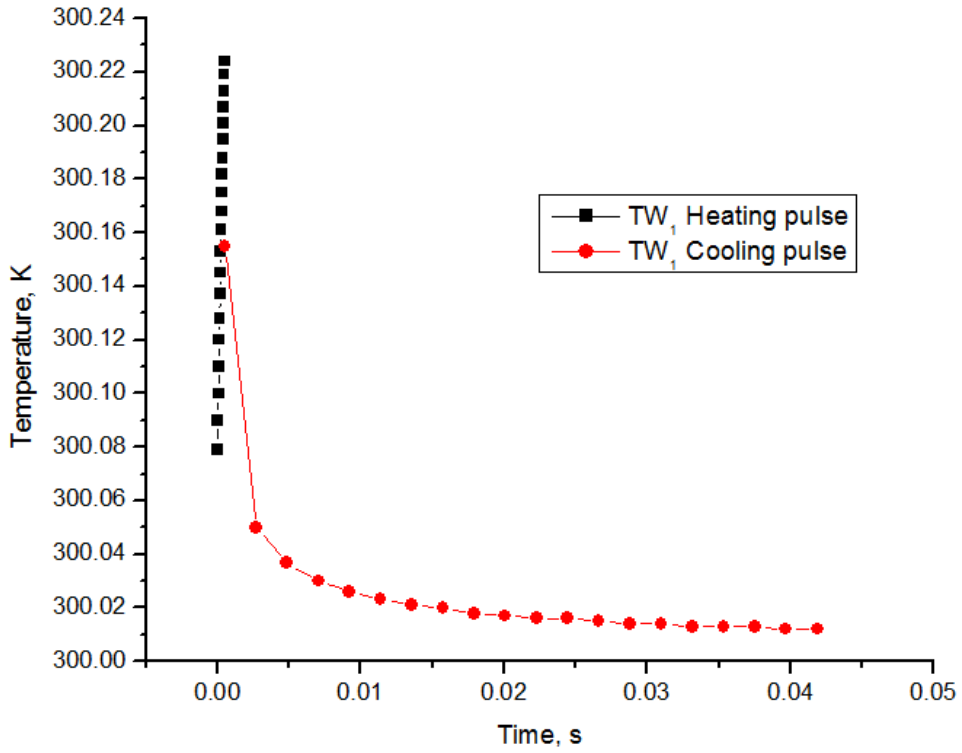

Figure 3.3. Variation in temperatures along the inner wall (TW_1) during one cycle

Figures 3.4 and 3.5 show the temperature distribution along the outer wall during heating and cooling pulse. The figures show that there is no temperature rise along the surface. There is no temperature rise for the outer wall (TW_2) even during heating pulse since it is estimated at one cycle and the residence time of detonation wave is only microseconds. In addition the outer wall is in contact with the coolant. The same approximation can be made for all the three stoichiometric mixtures.

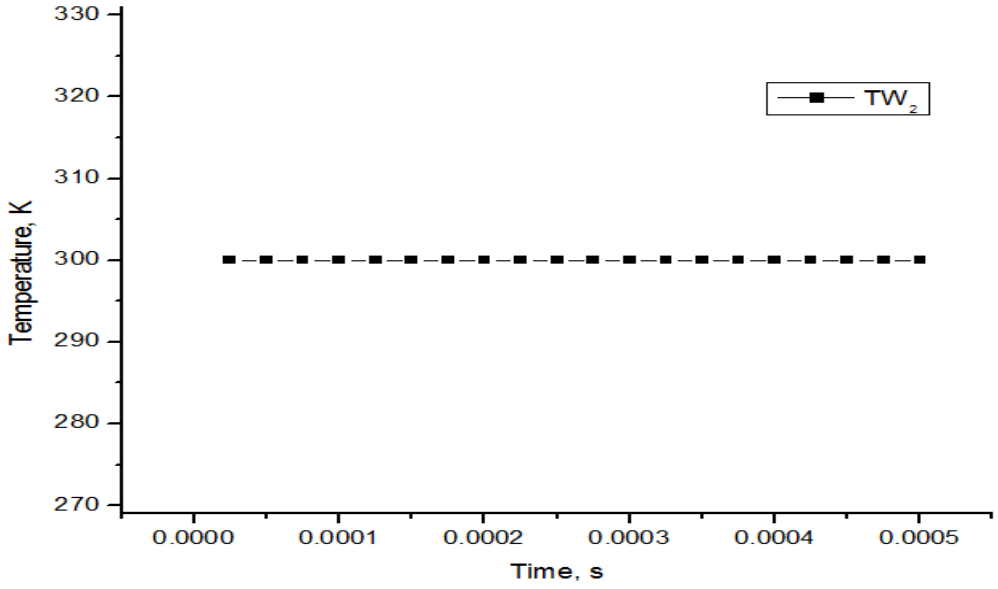

(a)

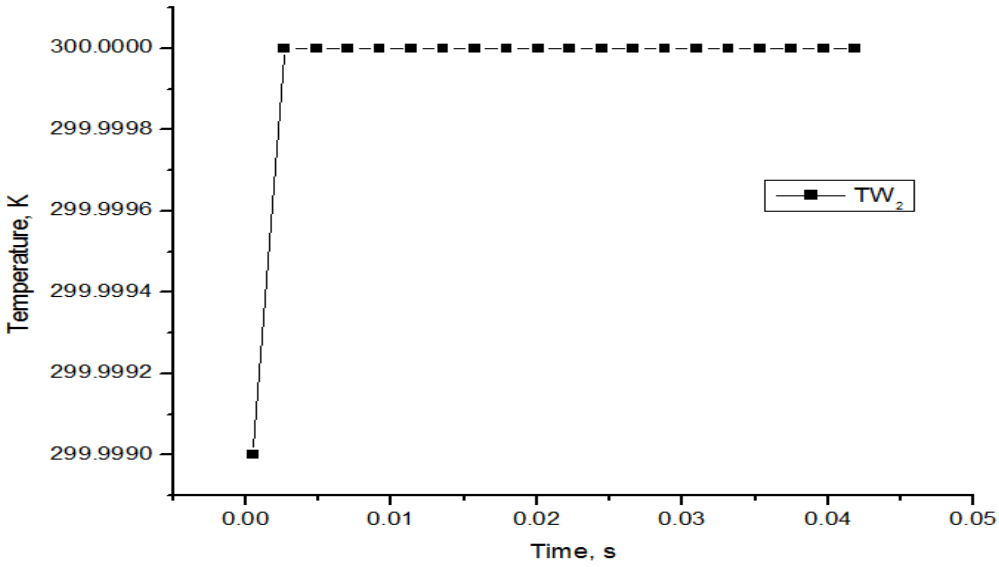

(b)

Figure 3.4. Variations in temperature along outer wall (TW_2) for np=1 (a) heating pulse and (b) cooling pulse

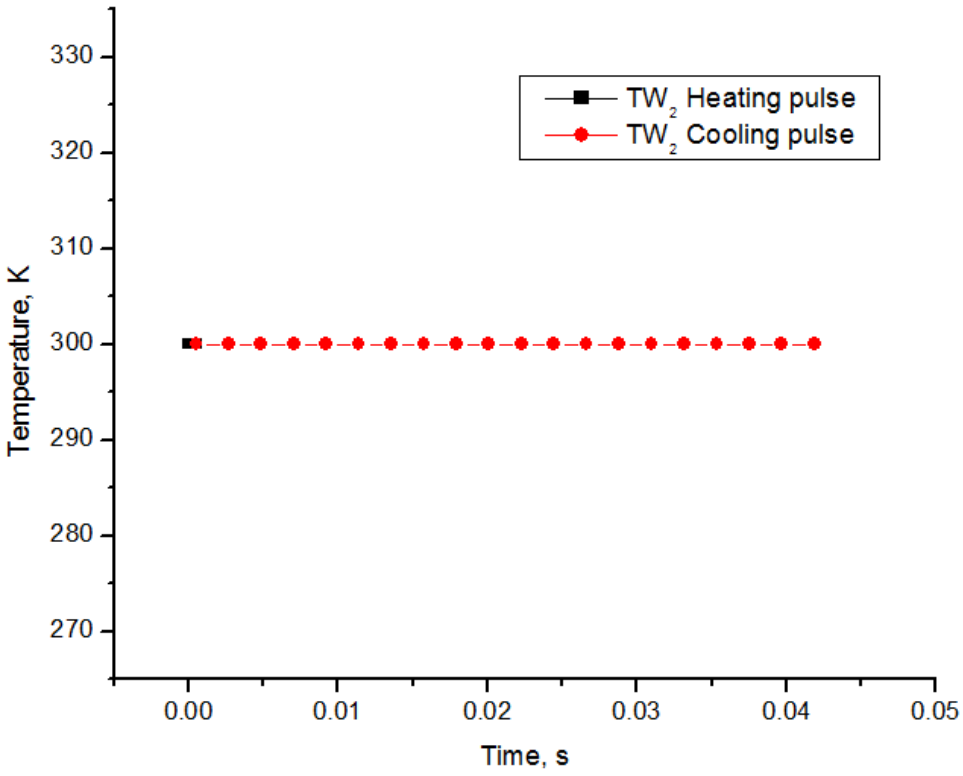

Figure 3.5. Variation in temperatures along the outer wall (TW_2) during one cycle

3.4.2 Octane and Air

The input data to the Mathematica code in this case is

a) $\mathrm{q} = 613695\ \mathrm{W/m^2}$

b) $\mathrm{h} = 2190\ \mathrm{W/m^2\,K}$

c) $\mathrm{np} =$ number of cycles

d) $\mathrm{t_p} = 0.00055\ \mathrm{s}$ [detonation time]

e) $\mathrm{t_{end}} = 0.04358\ \mathrm{s}$ [total cyclic time]

f) $r_i = 0.05\ m$

g) $r_0 = 0.07\ m$

The differences in the input for the Mathematica in this case when compared with that for hydrogen/air are the heat flux, detonation time and total cyclic time.

Figure 3.6 shows the comparison of heating pulse along the inner and outer surfaces and Figure 3.7 shows the comparison of cooling pulse along the surfaces for octane/air. Though the heat release per unit area is more for the stoichiometric mixture of octane/air, the temperature does not increase much for one cycle along the inner surface. Also the outer surface temperatures are almost the same when compared with hydrogen/ air. The inner wall reaches to a temperature of 300.5K for octane/air for one detonation wave propagation and comes down to 300 K towards the end of the cycle. Figure 3.8 clearly shows the temperature distribution along the inner and outer walls for single cycle for the stoichiometric mixture of octane/air.

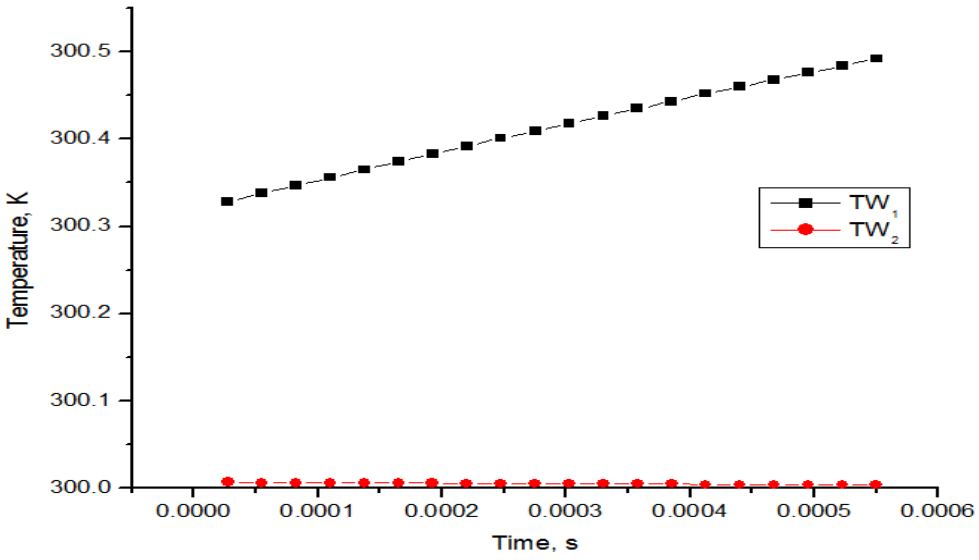

Figure 3.6. Comparison of inner surfaces of one heating pulse for octane/air

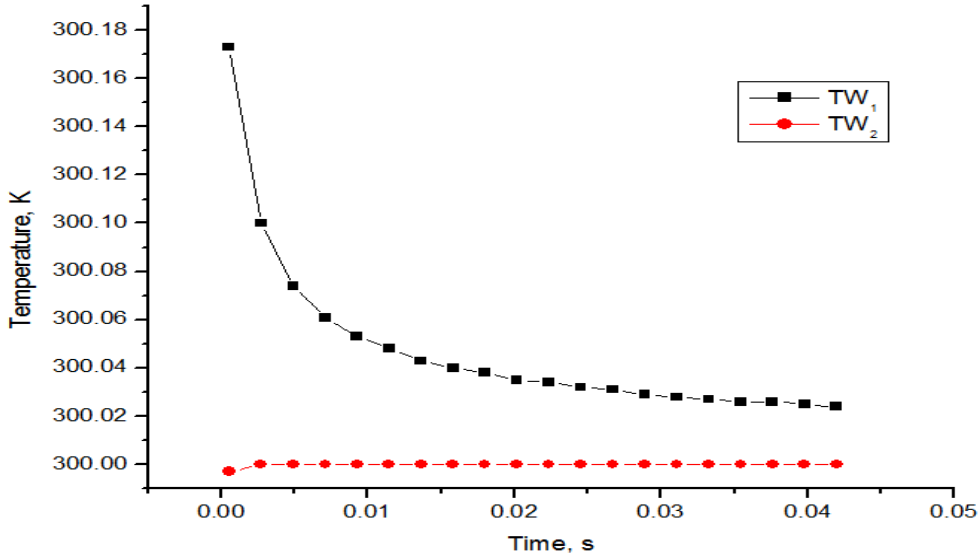

Figure 3.7. Comparison of outer surfaces of one cooling pulse for octane/air

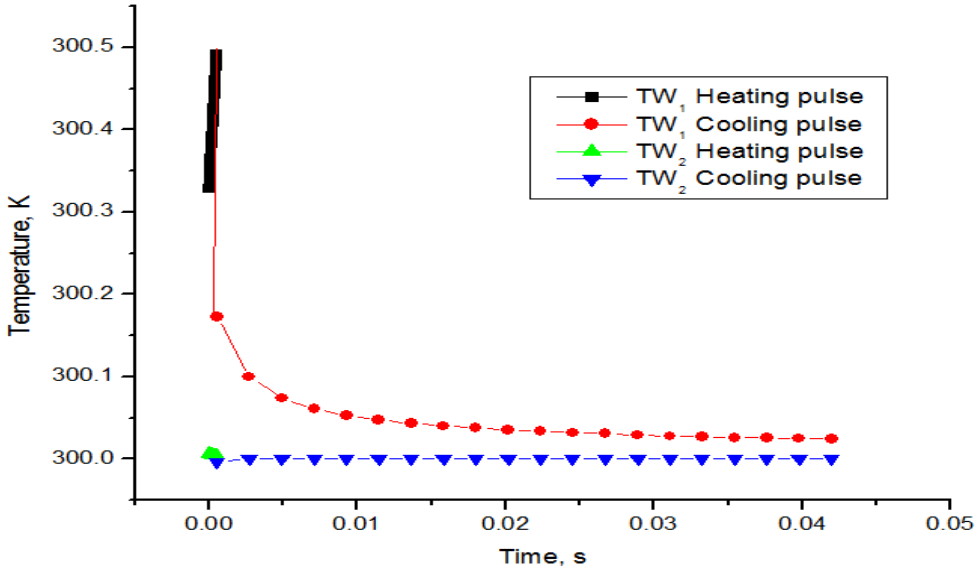

Figure 3.8. Variation in temperature for one cycle along inner and outer surfaces for octane/air

3.4.3 Octane and Oxygen

The input data to the Mathematica code in this case is

a) $\mathrm{q} = 1049364\ \mathrm{W/m^2}$

b) $\mathrm{h} = 2190\ \mathrm{W/m^2\,K}$

c) $\mathrm{np} =$ = number of cycles

d) $\mathrm{t_p} = 0.00043\ \mathrm{s}$ [detonation time]

e) $\mathrm{t_{end}} = 0.04353\ \mathrm{s}$ [total cyclic time]

f) $r_i = 0.05\ m$

g) $r_0 = 0.07\ m$

Figure 3.9 clearly shows the temperature distribution along the inner and outer walls for single pulse for the stoichiometric mixture of octane/oxygen

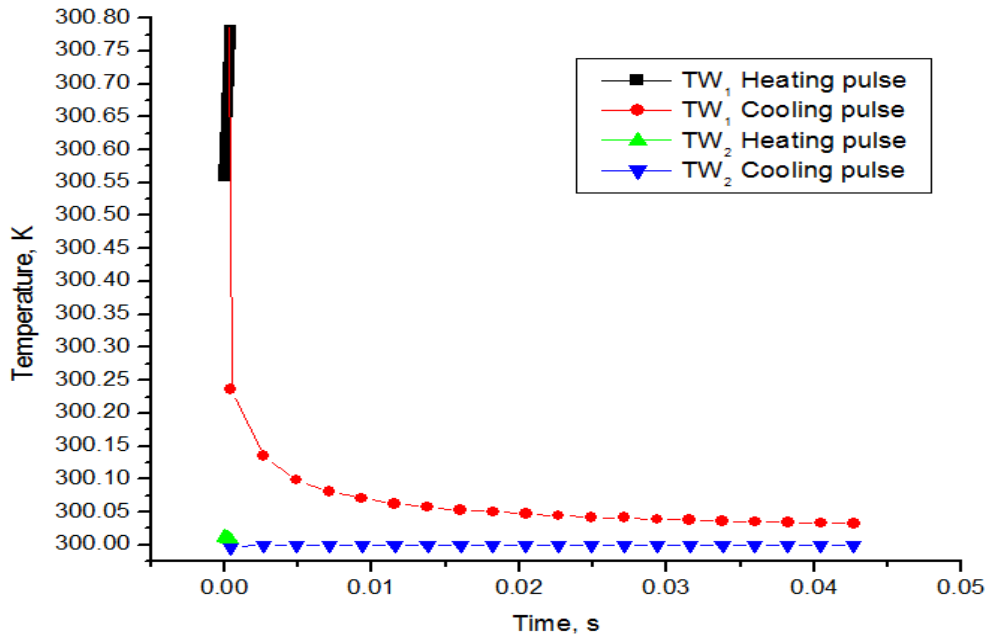

Figure 3.9. Variation in temperatures for one cycle along inner and outer walls for octane/oxygen

3.4.4 Comparison of Heating and Cooling Pulse Profiles for Three Stoichiometric Mixtures

Figures 3.10 and 3.11 show the profiles during heating and cooling pulse for stoichiometric mixtures of hydrogen/Air, octane/air and octane/oxygen for one cycle. It can be approximated that the heating and cooling pulse profiles look the same for increasing number of cycles also. It means the heating and cooling pulse profiles at np=3000 also looks the same with the only difference being the temperature levels. A clear comparison of temperature distribution for one complete pulse along the inner and outer surface is shown in Figure 3.11.

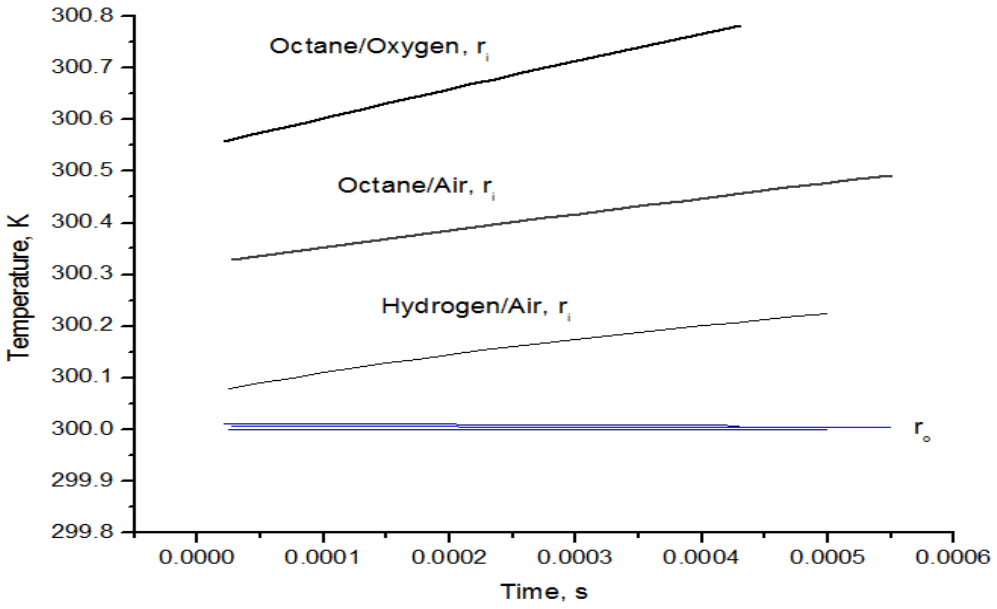

Figure 3.10. Inner and outer surface profiles for three stoichiometric mixtures for one heating pulse

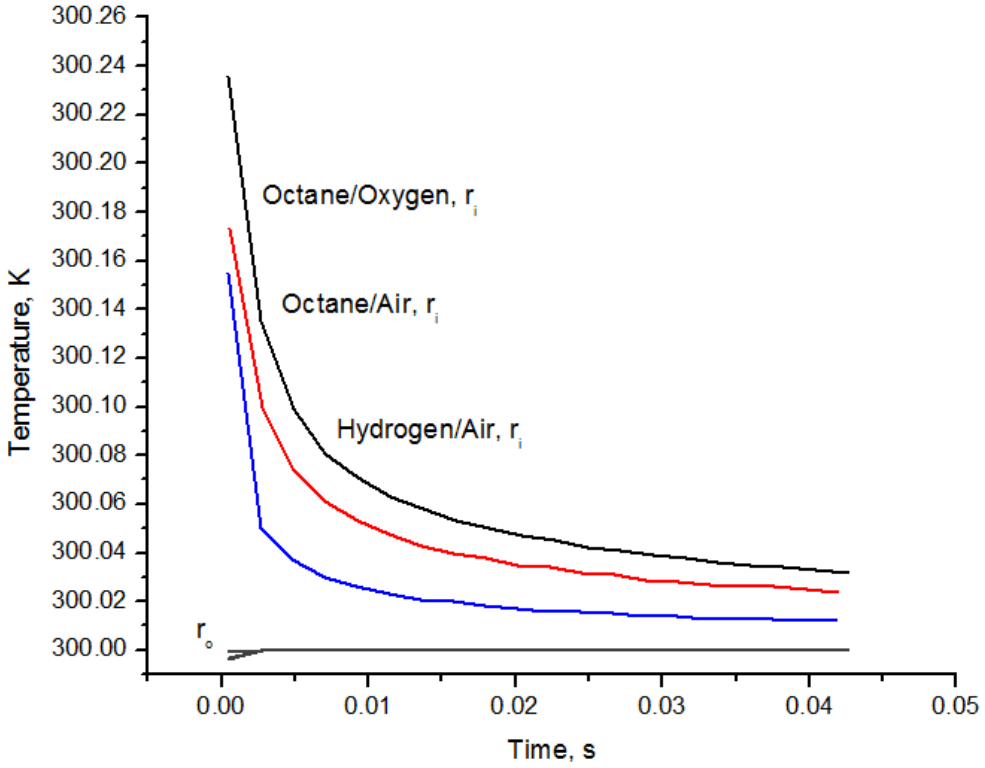

Figure 3.11. Inner and outer surface profiles for three stoichiometric mixtures for one cooling pulse

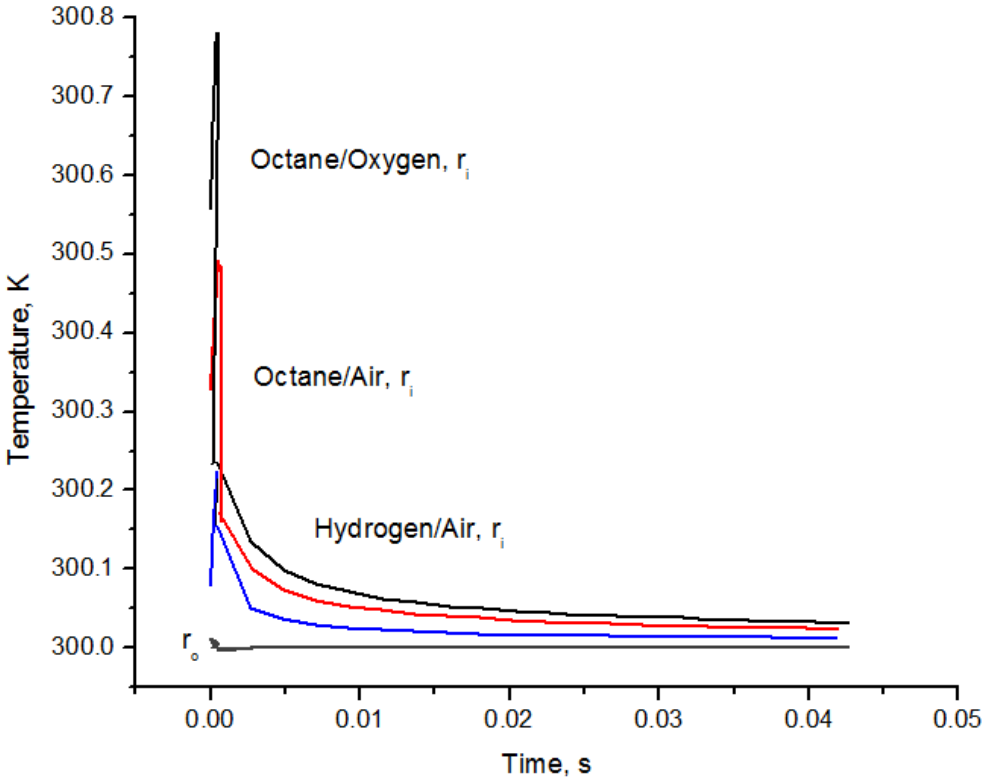

Figure 3.12. Inner and outer surface profiles for three stoichiometric mixtures for one pulse

3.5 Calculation of Wall Temperatures for Large Number of Cycles

3.5.1 Hydrogen and Air

The same input is given to the Mathematica code but the number of pulses is increased till 7000 cycles to observe how the walls are affected. Figure 3.13 shows how the temperature of the inner wall varies with increasing pulses for hydrogen/air. It can be observed that the temperature becomes almost steady after 3000 pulses. The inner wall temperature TW_1 reaches only to 301.6 K after 3000 pulses and then slowly rises. The low temperature is because of space-time averaging throughout the length of the tube.

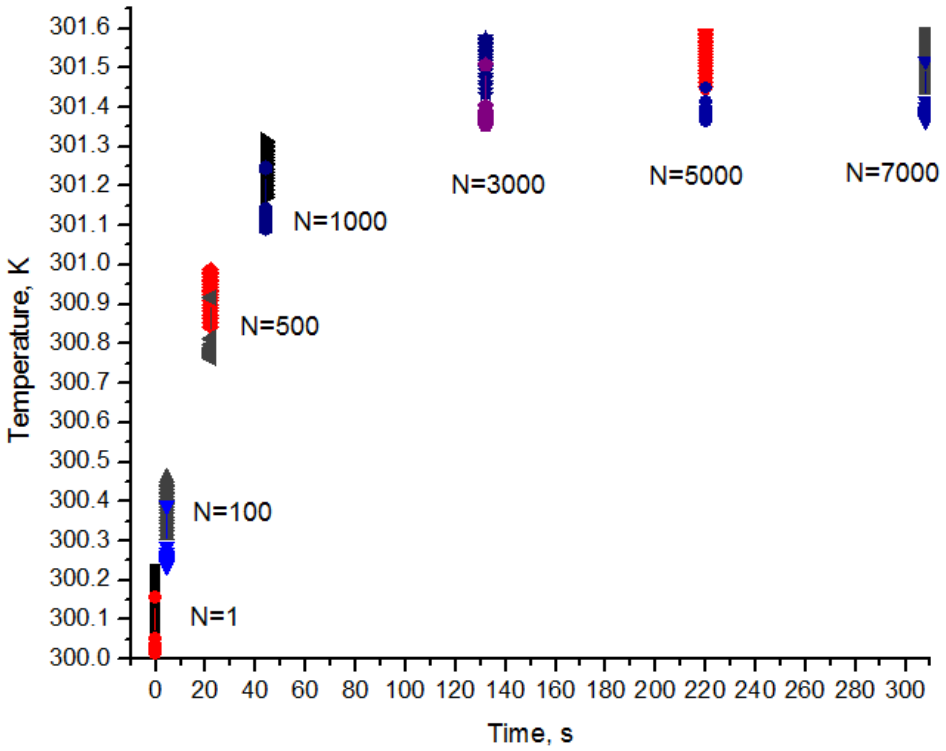

Figure 3.13. Inner surface temperature profiles with number of pulses

The variations in temperature along the outer wall for increasing pulses is shown in Figure 3.14. Not much difference can be observed between the heating and cooling pulse along the outer wall when compared with inner wall temperature profiles. The outer wall still remains at 300K after 3000 cycles.

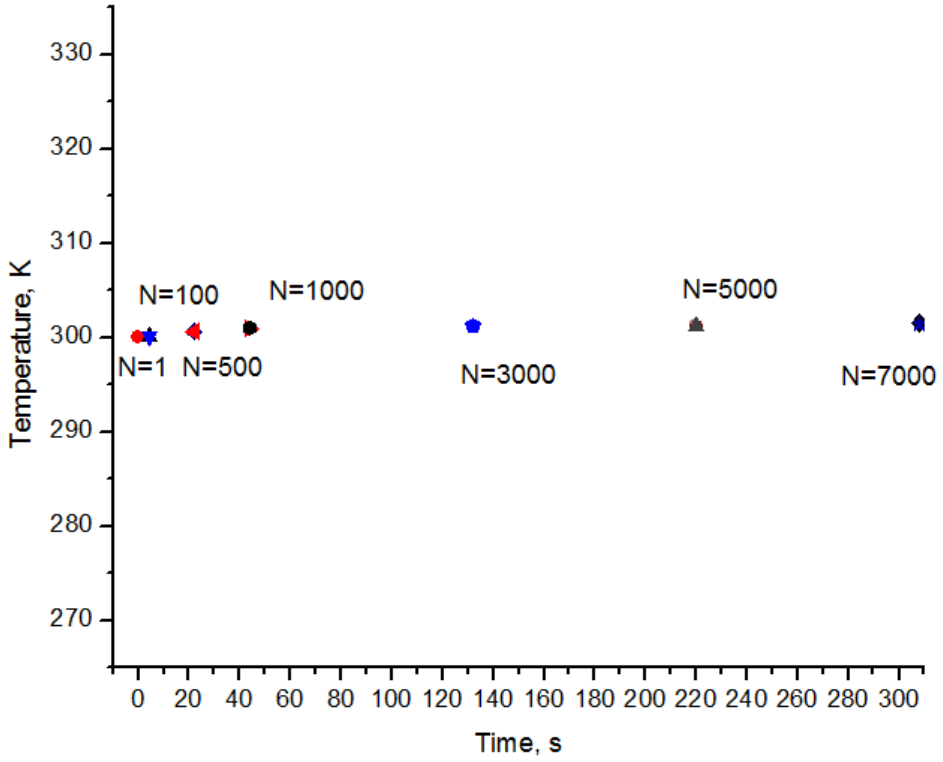

Figure 3.14. Outer surface temperature profiles for increasing pulses

3.5.2 Octane and Air

The same input is given to the Mathematica code as discussed for one cycle for octane/air but the number of pulses is increased till 7000. Figure 3.15 shows the temperature distribution along the inner and outer wall for the detonation tube. Since the calculated heat release per unit area is much more compared with hydrogen/air, the wall temperatures are expected to be higher. The inner wall temperature TW_1 still reaches only to 303.5 K after 3000 cycles and then slowly rises before steadying. And the outer wall temperatures are at atmospheric conditions.

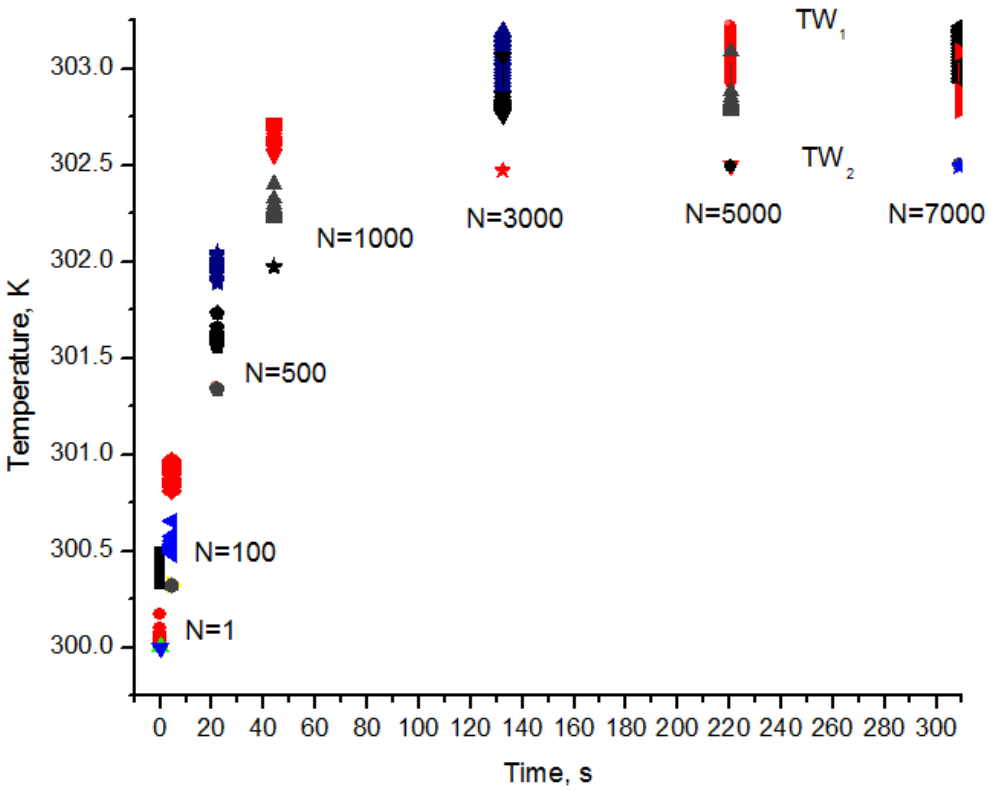

Figure 3.15. Inner and outer surface temperature profiles for increasing pulses for octane/air

3.5.2 Octane and Oxygen

The temperature distribution for octane/oxygen along the inner and outer wall is shown in Figure 3.16. The temperature reaches only to 304 K after 3000 cycles and becomes steady. Though the calculated heat release per unit area is much higher than other stoichiometric mixtures the temperature does not increase along the surfaces of the detonation tube.

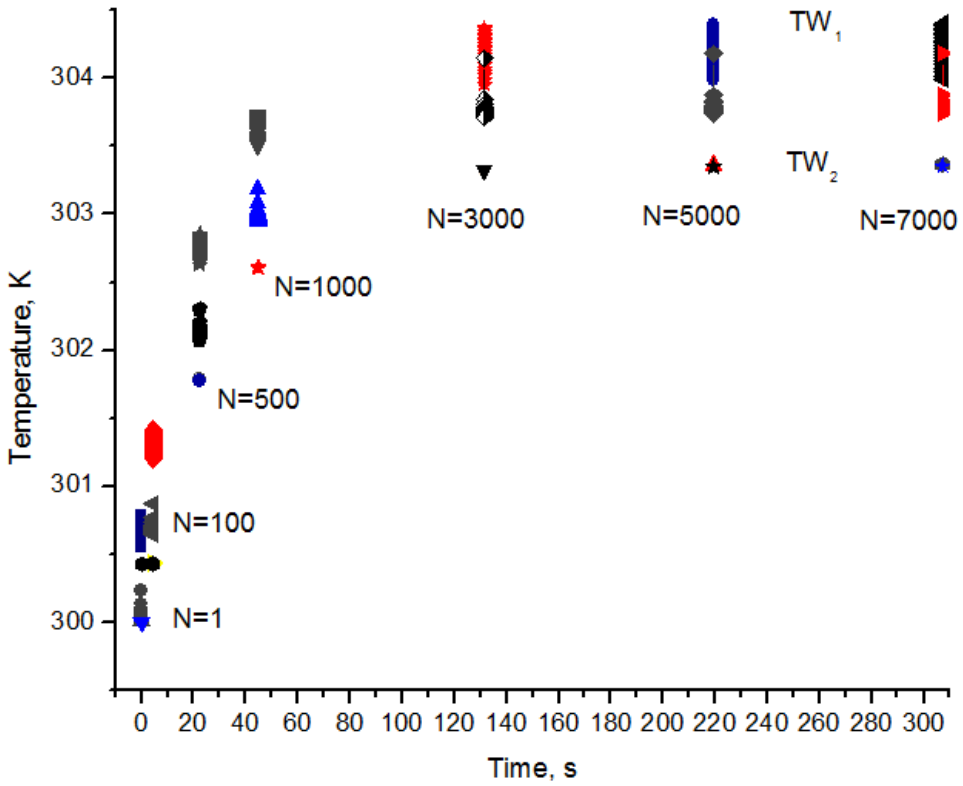

Figure 3.16. Inner and outer wall temperature profiles for increasing pulses for octane/oxygen

In summary, it can be deduced from the results that the temperature increases very slowly initially along the walls and slows down much with increasing time. After 3000 cycles the temperature along the inner and outer surfaces becomes almost steady for all the three stoichiometric mixtures.

CHAPTER 4

CONCLUSION AND DISCUSSION OF RESULTS

4.1 Conclusion

Heat transfer analysis of a 1 m long and 100 mm bore detonation tube with detonation pulses of 20 Hz cooled by a water jacket, was performed for stoichiometric mixtures of hydrogen/air, octane/air and octane/oxygen.

The research and study of pulse detonation engine has been accomplished by the following calculations.

1. The properties of temperature, pressure and density during detonation, rarefaction and exhaust processes.
2. The total heat generated during one cyclic operation.
3. Determination of wall temperatures TW_1 and $TW_2$for a detonation tube made of copper for multiple cycles.

The sensible heat release in a detonation tube was determined using the steady state energy equation for the three stoichiometric mixtures. This heat release was then used in the thermodynamic cycle analysis using transient heat conduction through hollow cylinders to determine the maximum theoretical performance. A brief study on the property distribution inside the walls of the detonation tube for multiple cycles was presented. The obtained values can be used for the preliminary heat exchanger design with the material selection.

4.2 Results and Discussion

Based on the results, it is concluded that though the temperatures are expected to be high along the surfaces of the detonation tube, due to space-time averaging procedure the temperature level does not rise much along the inner wall. And also the outer wall almost remained at 300 K for the three stoichiometric mixtures. The temperature becomes almost steady after 3000 cycles. The results found in this study give some indication of heat load on the walls of the detonation tube and indicate that PDEs can be operated at higher frequencies.

4.3 Recommendations

Future work can be focused on different models with inlets and nozzles since the results of cooled wall heat load measurements are applied for simple straight tubes. Since the present analysis is carried as a ground demonstrator, water is used as a coolant. The same analysis can be performed for other coolants with different flow rates and with different material selection like steel and Haynes alloy which can withstand high temperatures. One should also take into account the weight of the engine which is a primary factor for any flight demonstration.

APPENDIX A

CEA CODE – INPUT AND OUTPUT

Chemical equilibrium application (CEA)[13,14] is a program developed by NASA which calculates thermodynamic and transport properties for the product mixture for any given set of reactions.

Input to CEA code for the three stoichiometric mixtures of hydrogen/air, octane/air and octane/oxygen is the temperature =298.15 K and pressure= 1 atm.

A.1 Output from CEA code for burned gases for different stoichiometric mixtures

Thermodynamic Properties	Hydrogen/Air	Octane/Air	Octane/Oxygen
$\mathrm{p, atm}$	15.38	18.392	38.816
T, K	2942.69	2833.59	3908.00
$\rho,\ \mathrm{kg/m^3}$	1.5290-3	2.2357-3	2.9169-3
$\mathrm{H, cal/g}$	318.62	241.40	413.05
$\mathrm{U, cal/g}$	75.029	42.165	90.784
$\mathrm{M, 1/n}$	24.007	28.264	24.099
$\mathrm{C_p,\ J/kg\ K}$	0.8029	0.6541	2.0718
γ	1.1636	1.1649	1.1378
$\mathrm{v, m/s}$	1089.0	985.4	1238.6
$\mathrm{visc, millipoise}$	0.92482	0.88468	1.1931
$\mathrm{M_{CJ}}$	4.8315	5.4019	8.0438
$\mathrm{D_{CJ}, m/s}$	1964.8	1785.9	2299.5

REFERENCES

1. McManus, K., Furlong, E., Leyva, I., Sanderson, S., MEMS - Based Pulse Detonation Engine for Small-Scale Propulsion Applications, AIAA-2001-3469, 2001.
2. Hoke, J., Bradley, R., Schauer, F., Heat Transfer and Thermal Management in a Pulsed Detonation Engine, AIAA Paper 2003–6486, 2003.
3. Ajmani, K., Breisacher, J.K., Multi- Cycle Analysis of an Ejector-Cooled Pulse Detonation Engine, AIAA 2004-3915, 2004.
4. Ciccarelli, G., Card, J., Detonation in Mixtures of JP-10 Vapor and Air, AIAA Journal, Vol. 44, No.2, February 2006.
5. Povinelli, L.A., Impact of Dissociation and Sensible Heat Release on Pulse Detonation and Gas Turbine Engine Performance, ISABE 2001-1212; also, NASA/TM–2001–211080.
6. Nagarajan, H. N., Lu, F.K., Preliminary Heat Exchanger Design for Pulse Detonation Engine, ISSN 1757- 2258.
7. Endo, T., Fujiwara, T., A Simplified Analysis on a Pulse Detonation Engine Model, Transactions of the Japan Society for Aeronautical and Space Sciences Vol. 44, No.146, pp. 217–222, 2002.
8. Endo, T., Fujiwara, T., Analytical Estimation of Performance Parameters of an Ideal Pulse Detonation Engine, Transactions of the Japan Society for Aeronautical and Space Sciences, Vol. 45, No. 150, pp. 249–254, 2003.
9. Mills, F.A., Basic Heat and Mass Transfer, Richard D Irwin, Inc., Chicago, 1995.

10. Kailasanath, K., Recent Developments in the Research on Pulse Detonation Engines, AIAA Journal, Vol. 41, No. 2, February 2003.
11. Li, S.C., Varatharajan, B., and Williams, F.A., Chemistry of JP-10 Ignition, AIAA Journal, Vol. 39, No. 12, pp. 2351-2356, 2001.
12. Haji Sheikh, A., Beck, J.V., Code, K.D. and Litkouhi, B., Heat Conduction Using Green's Functions, Hemisphere Publishing Corporation, 1992
13. McBride, B.J. and Gordon, S., Computer Program for Calculation of Complex Chemical Equilibrium Compositions and Applications I. Analysis, NASA-RP1311, October 1994.
14. McBride, B.J. and Gordon, S., Computer Program for Calculation of Complex Chemical Equilibrium Compositions and Applications II. User's Manual and Program Description, NASA-RP1311- P2, June 1996.

BIOGRAPHICAL INFORMATION

Neelima Kalidindi was born in 1986 in Bhimavaram but received her high school education in Hyderabad, Andhra Pradesh, India. She started her Bachelor of Engineering in 2003 at D.V.R College of Engineering and Technology, JNTU and received her degree of BE in 2007. Then, in 2008 she joined the University of Texas at Arlington to pursue her Master's. In 2009, she received her Master of Science in Mechanical Engineering and fulfilled her wish of specialization in this field.